Gaseous Detectors-1

IPMLHC2013: Second IPM Meeting on LHC Physics

TEHRAN Oct 7-11, 2013

Archana SHARMA

CERN Geneva Switzerland

Nuclear Instrumentation and Methods A, Volume 666, Pages 1-222 (21 February 2012)

Advanced Instrumentation
With all technologies used at LHC

Editor : Archana Sharma

http://www.sciencedirect.com/science/journal/01689002/666

Outline

- Introduction and fundamental principles
- Examples of Gaseous Detectors
- Aging and Long term Operation
- Talk 2: Upgrades with Gaseous Detectors (mostly CMS)

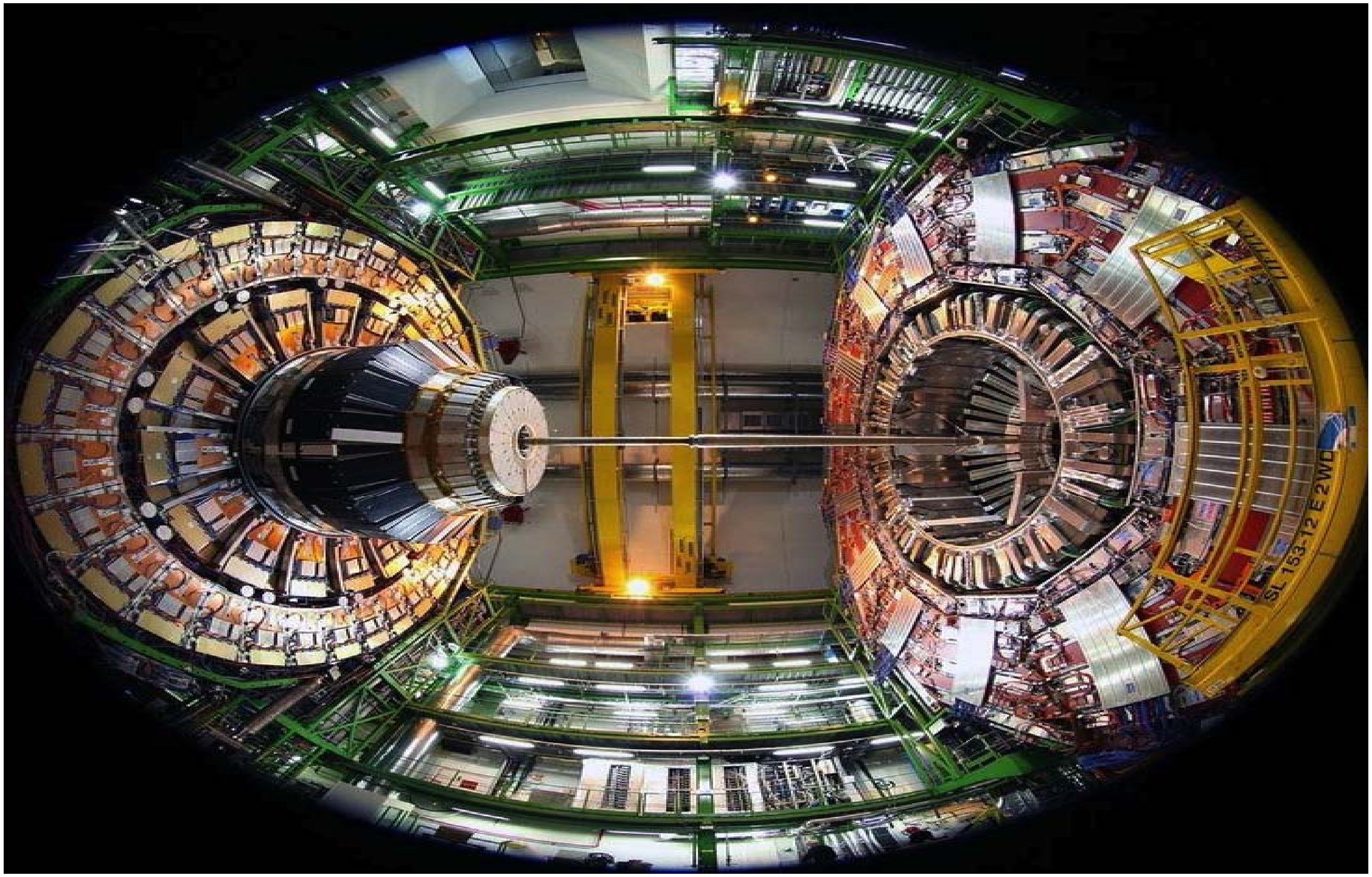

Gaseous Particle Detectors

Invented by Geor
Charpak
Nobel Prize -199

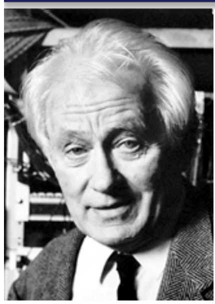

PRO
C

19

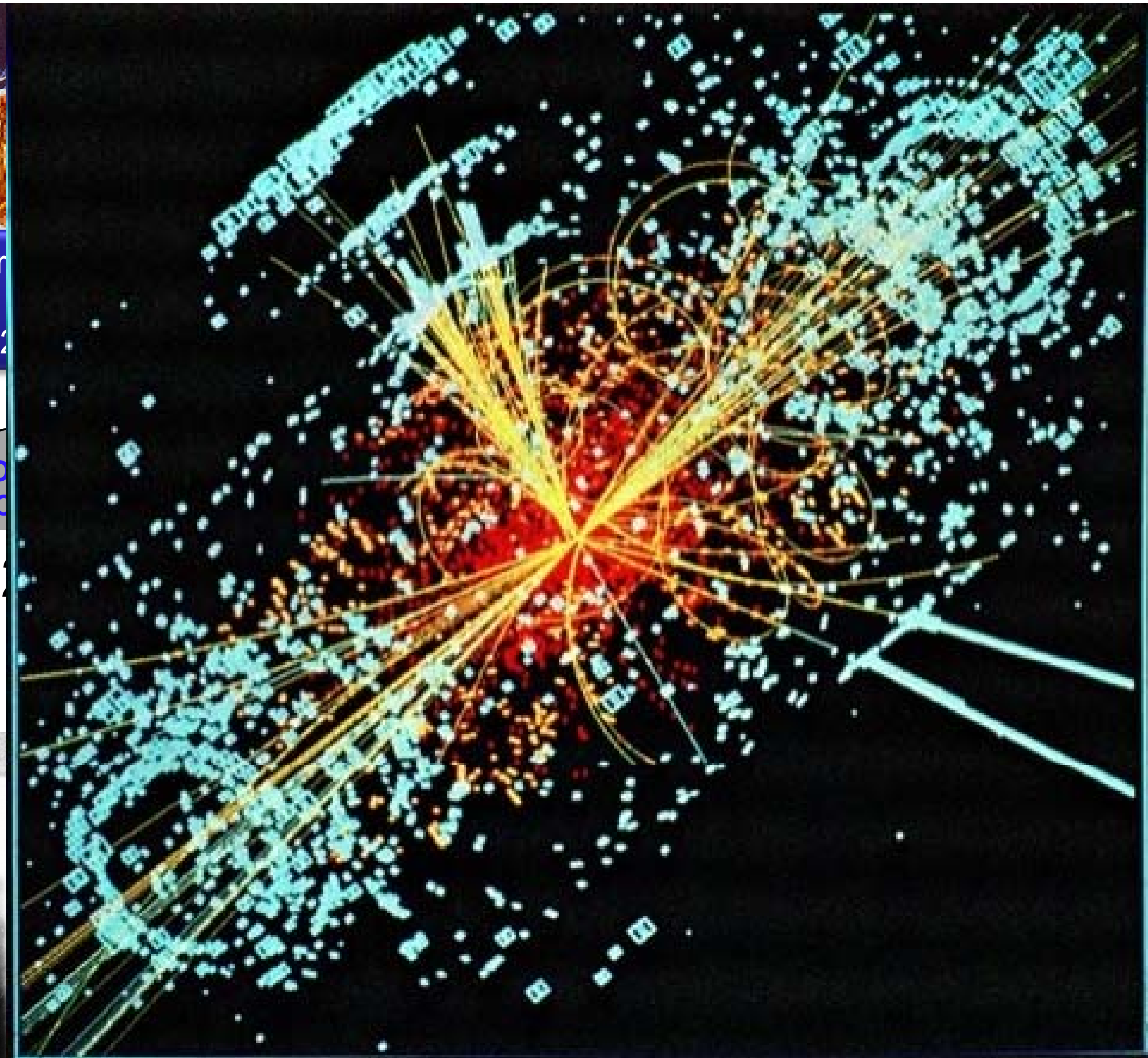

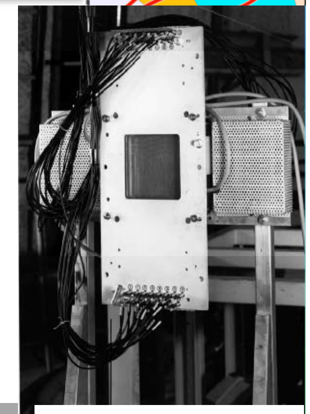

ON
IER

GAS

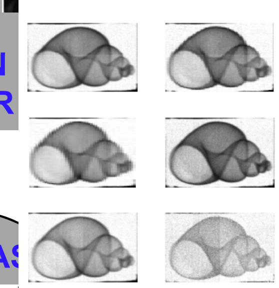

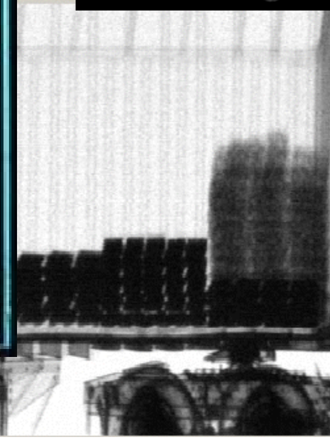

STATUS & EVOLUTION OF GASEOUS DETECTORS IN LAST TWO DECADES

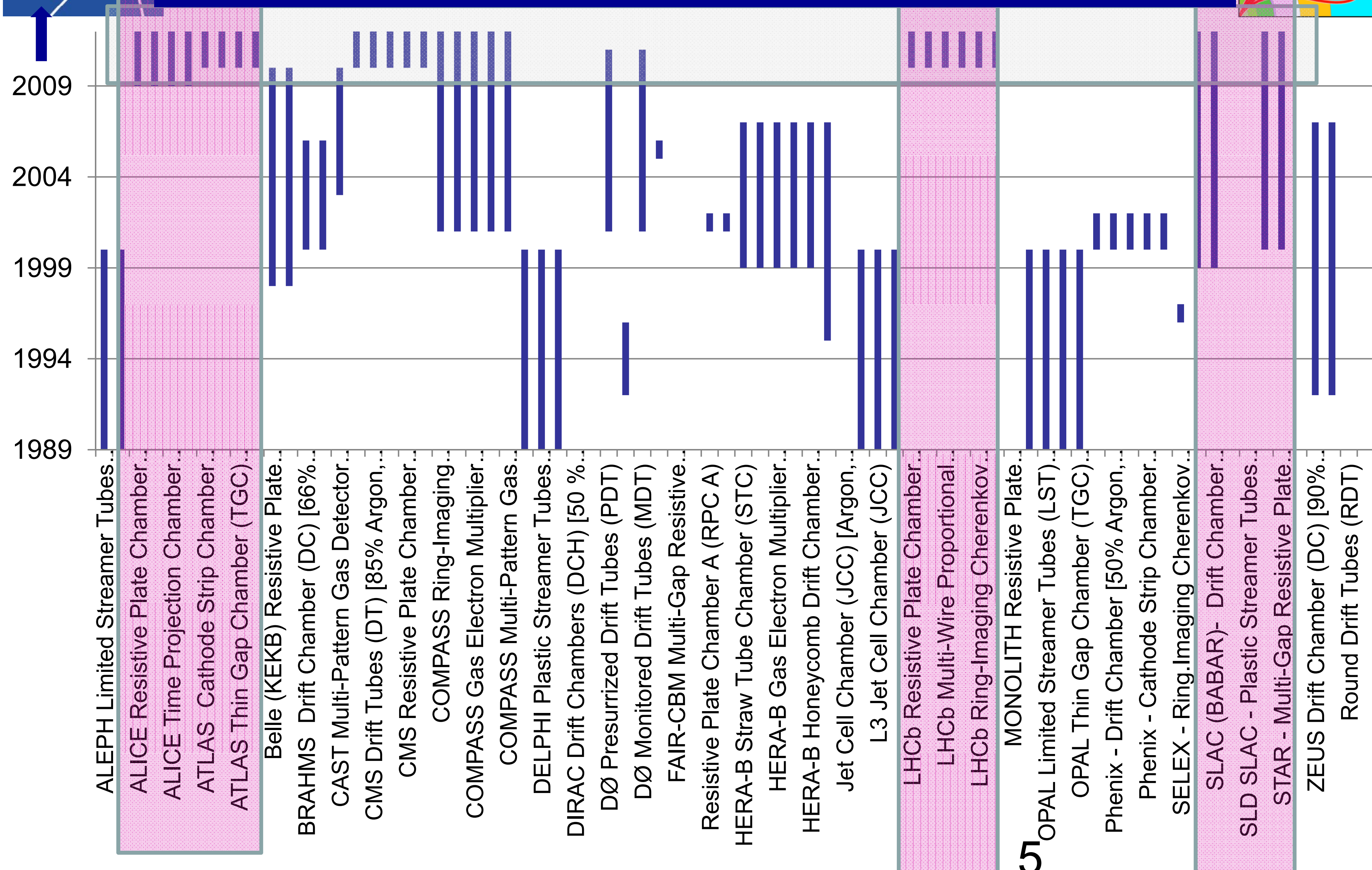

A. Sharma 2012

STATUS & EVOLUTION OF GASEOUS DETECTORS IN LAST TWO DECADES

See http://pdg.lbl.gov/atlas/index.html

See http://cmsinfo.cern.ch/Welcome.html/

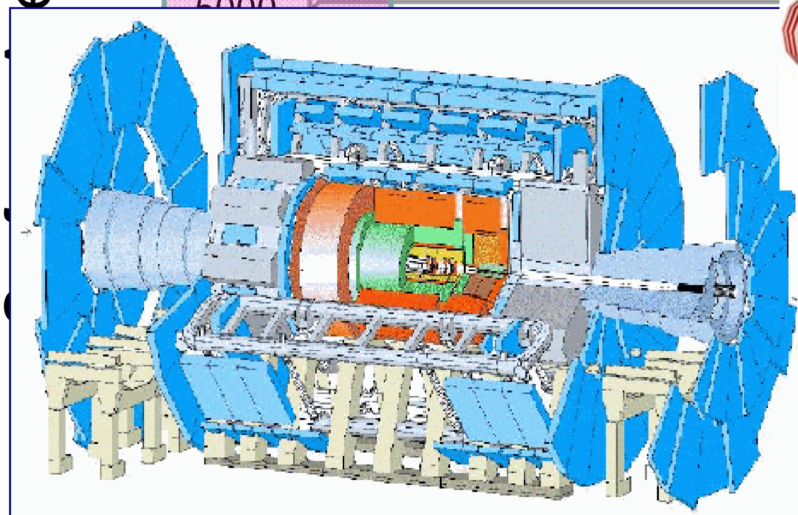

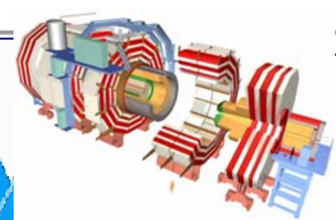

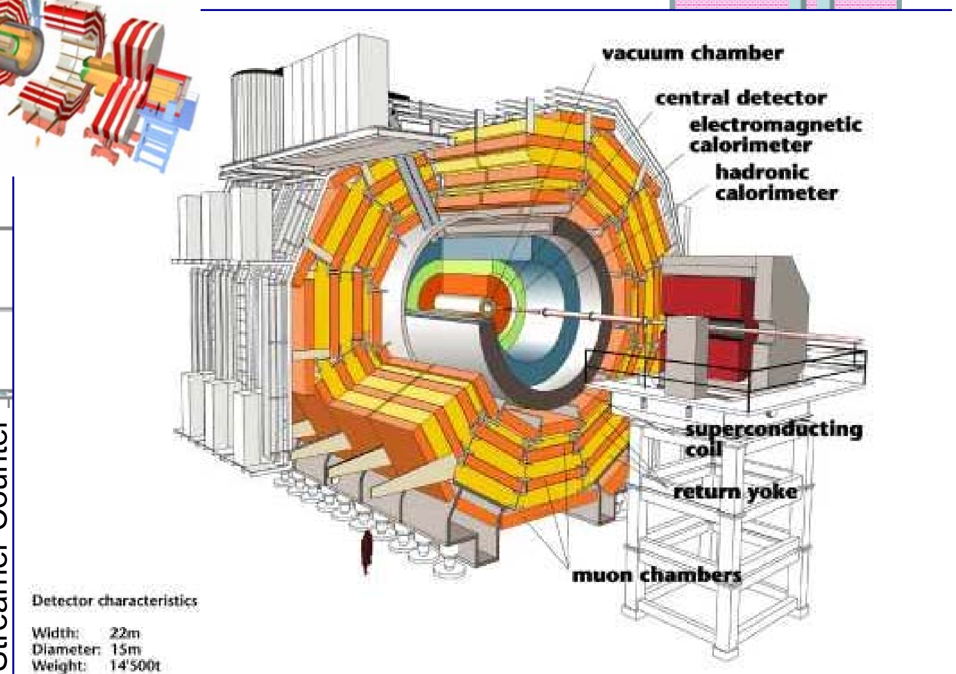

TOTAL
Gaseous Detectors
In ATLAS
~ 10,000 m^2

TOTAL
Gaseous Detectors
In CMS
~ 10,000 m^2

A. Sharma 2012

Principles of detection

Interaction of a particle with detector

Sensitive Material

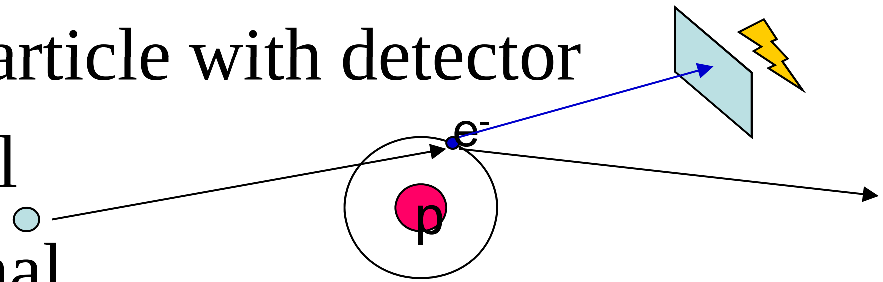

Measureable Signal

- Ionization
- Excitation

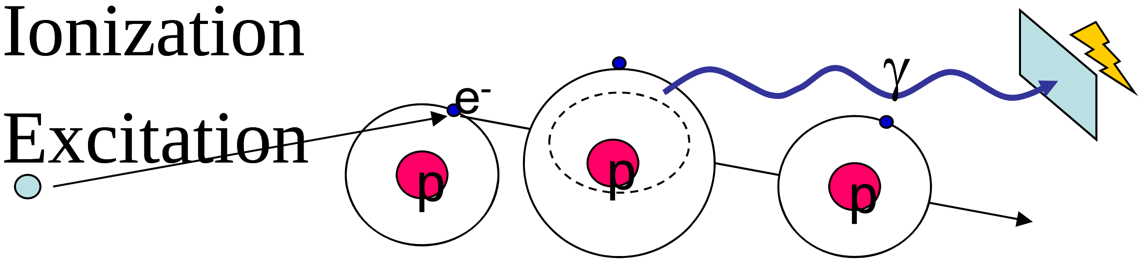

Particle trajectory is changed due to

Bending in a magnetic field, energy loss

Scattering, change of direction, absorption

Charge Generation in a Gas

Amount of ionization produced in a gas is not very great.

A minimum ionizing particle (m.i.p.) typically produces 30 ion pairs per cm from primary ionization in commonly used gases (e.g. Argon)

The total ionization is ~100 ion pairs per cm including the secondary ionization caused by faster primary electrons.

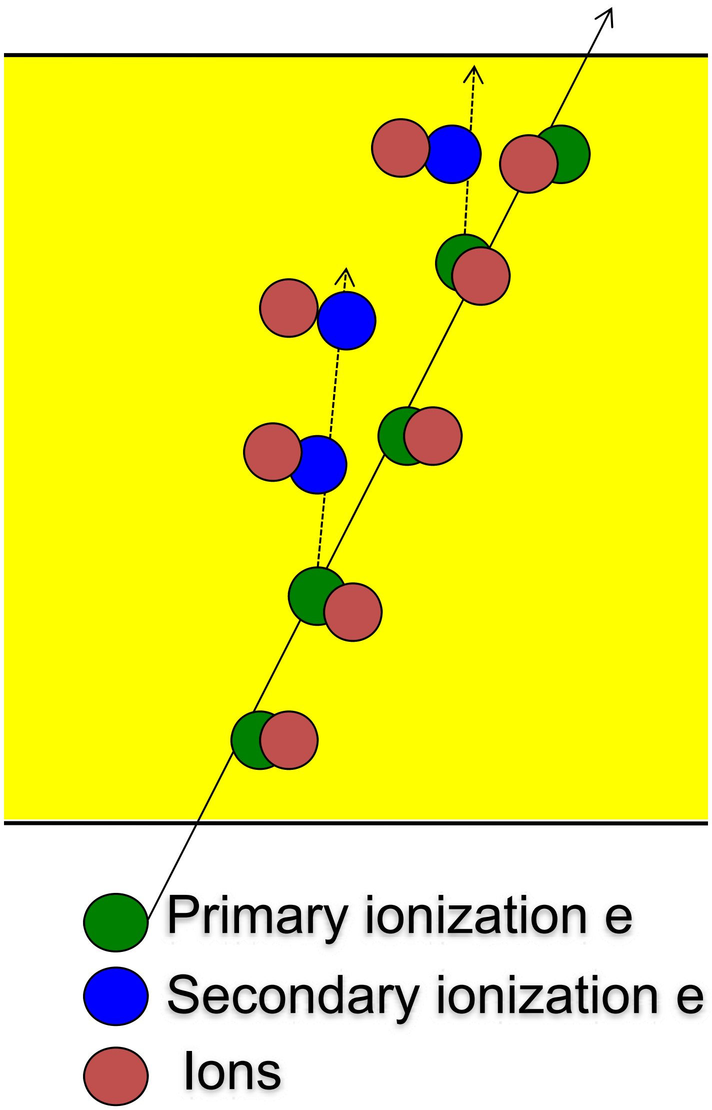

Charge Collection

Charge is produced near the track.

Apply an electric field to move charge to electrodes.

Charge is accelerated by the field, but loses energy through collisions with gas molecules.

Overall, steady drift velocity of electrons towards anode and positive ions towards the cathode.

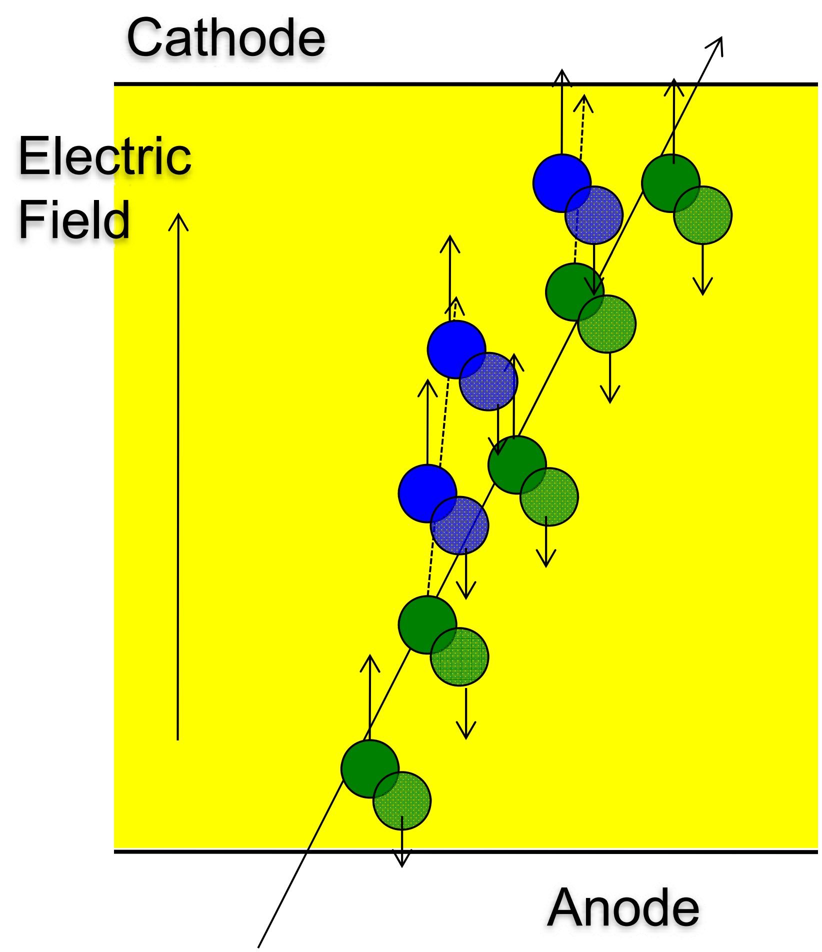

Ionization Chamber Geometry

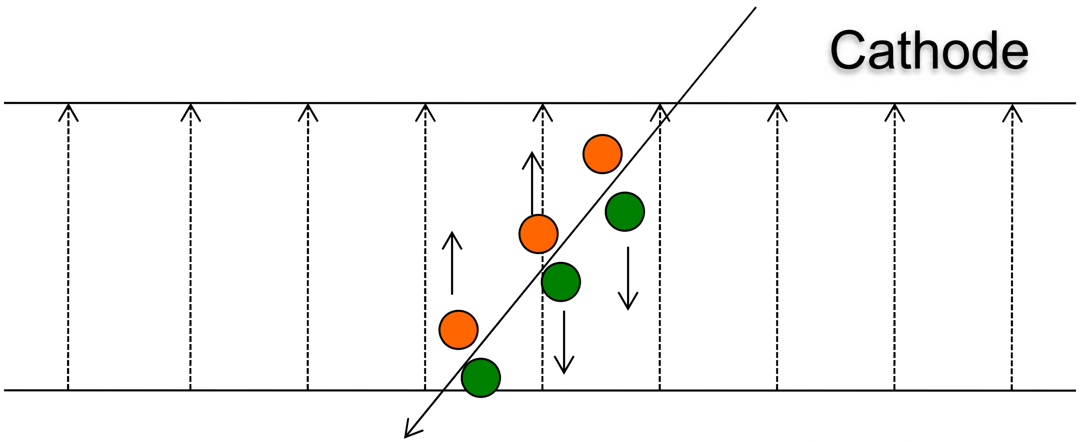

Parallel Plate Ionization Chamber

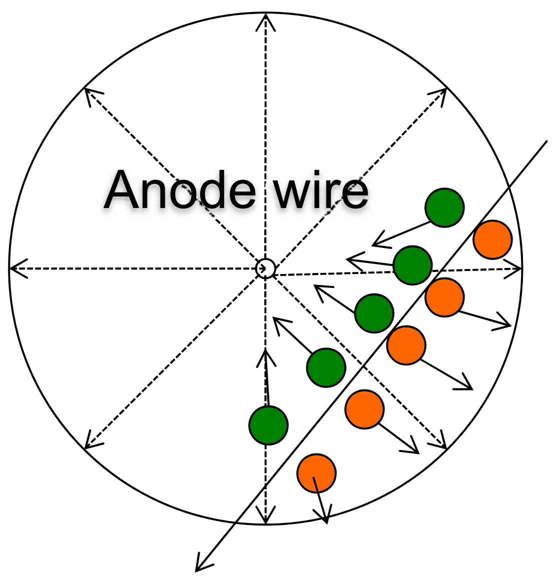

Cylindrical Ionization Chamber

WIRE PROPORTIONAL COUNTERS

Thin anode wire coaxial with cathode

Electric field:

$$E(r) = \frac{CV_0}{2\pi\varepsilon_0}\frac{1}{r} \qquad C = \frac{2\pi\varepsilon_0}{\ln(b/a)}$$

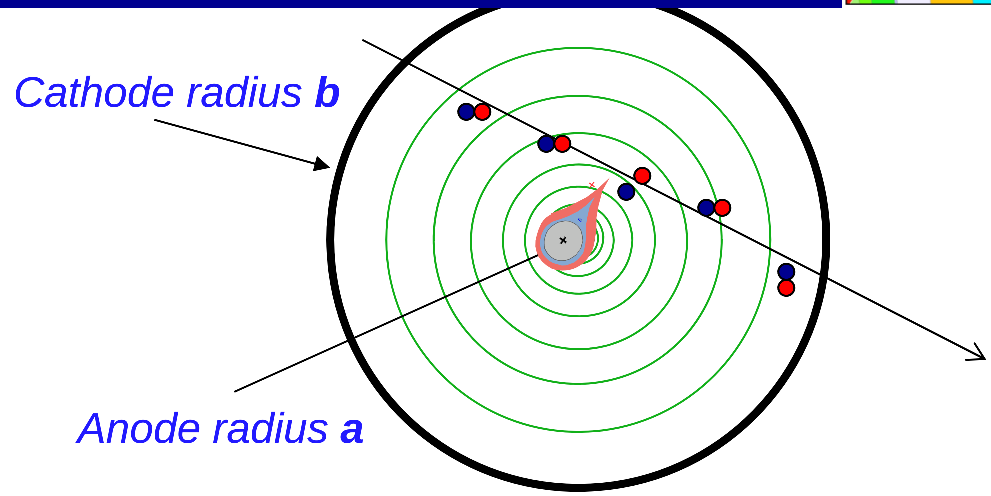

Avalanche development around a thin wire:

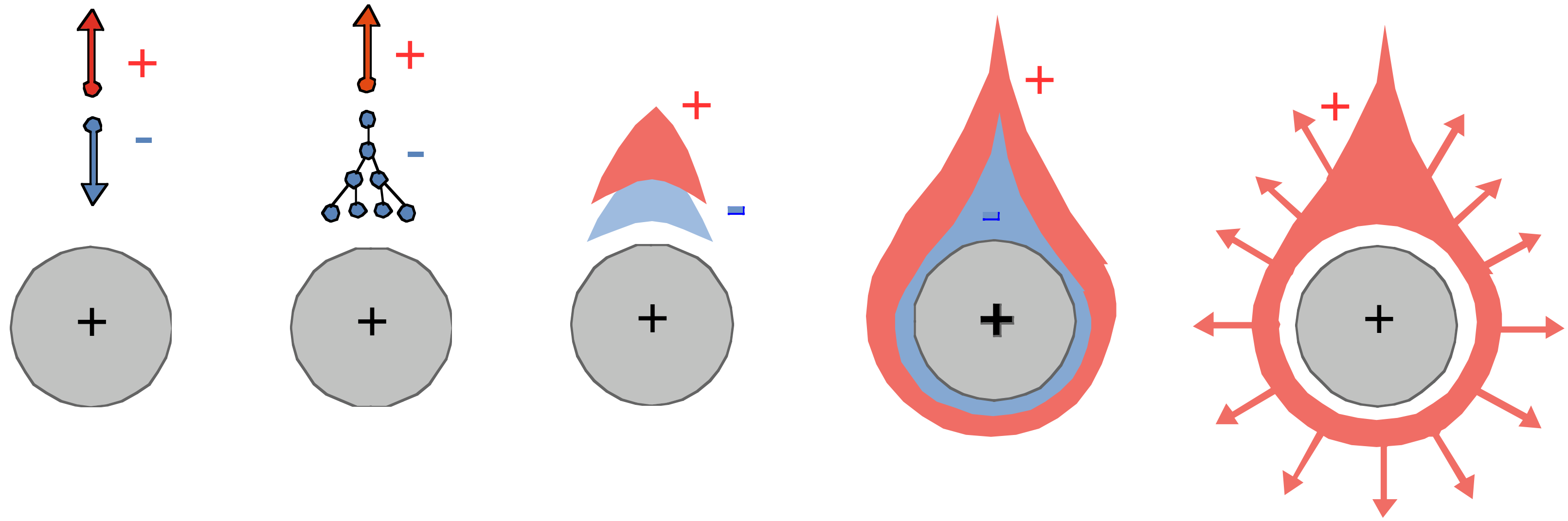

Multiwire Proportional Chamber

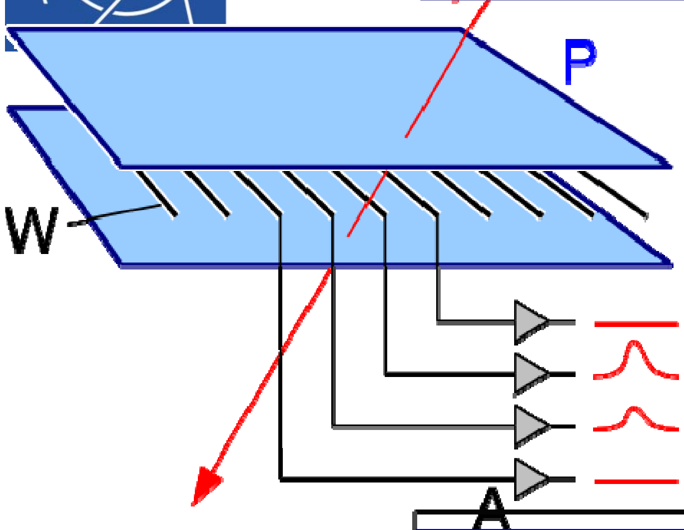

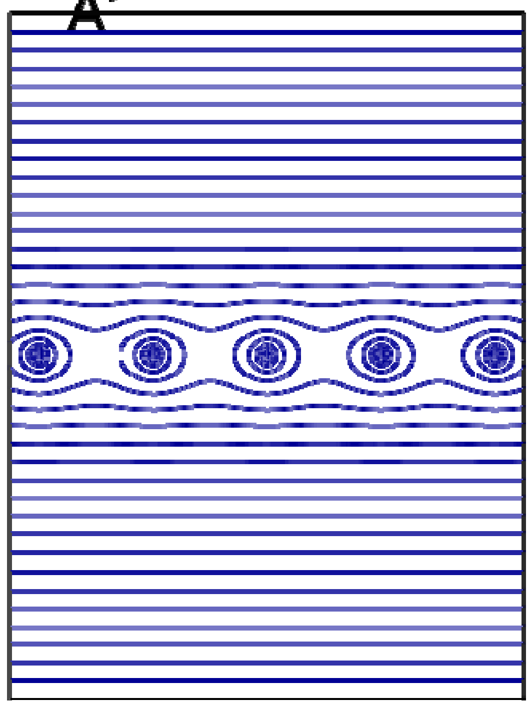

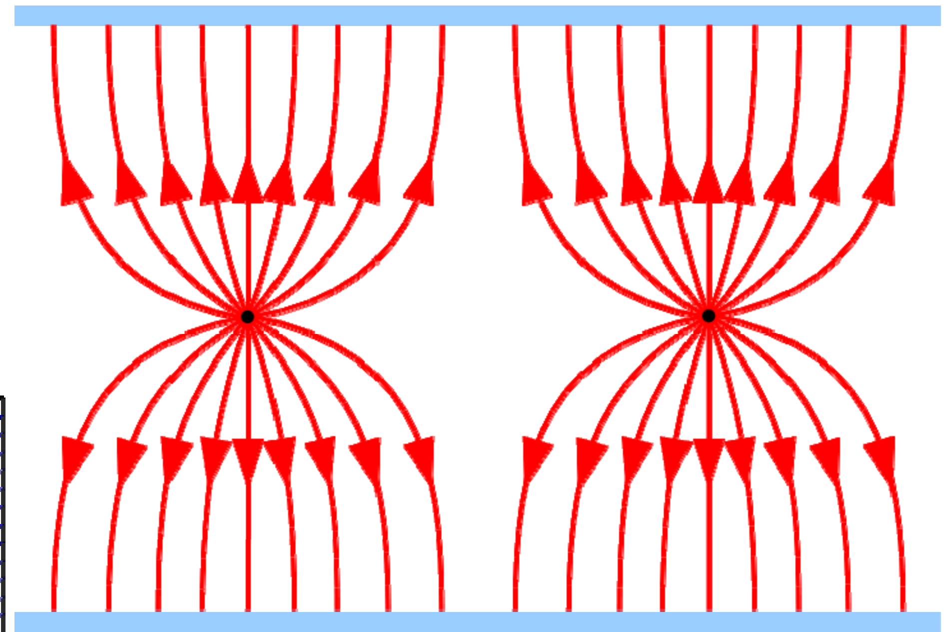

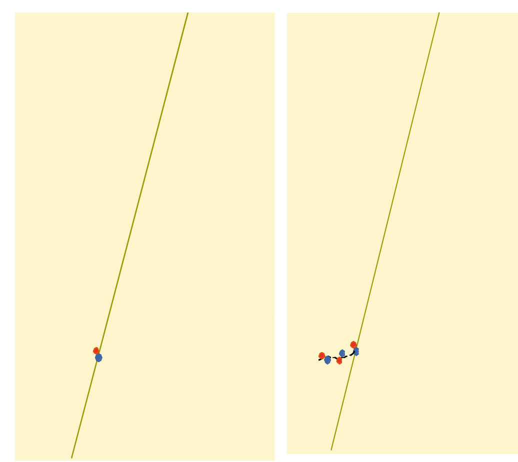

Multiwire Proportional Chamber (MWPC)

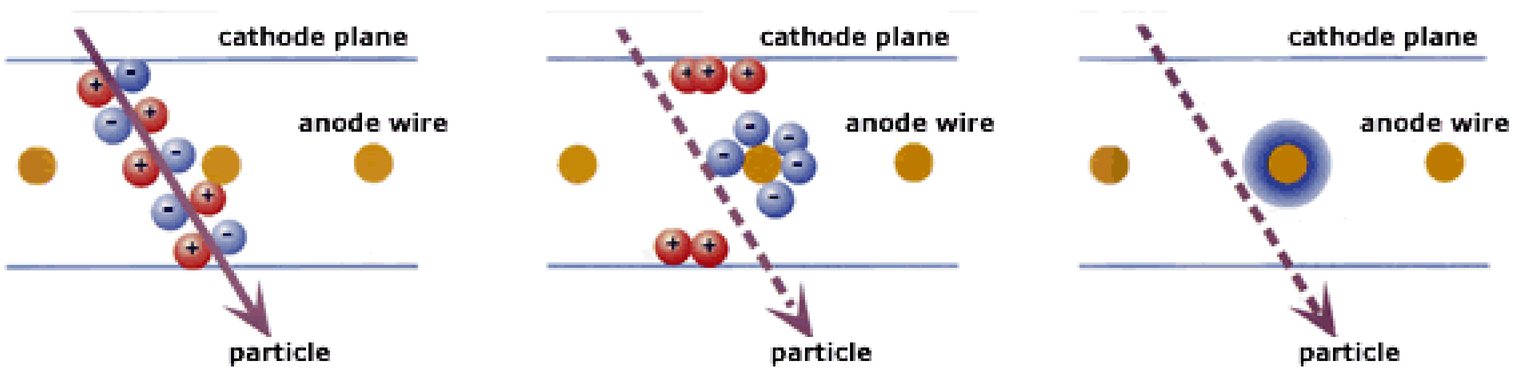

The particle ionizes the gas producing electrons and free ions.

The liberated electrons move rapidly move towards the anode wire and the ions towards the cathode plans

More electrons are liberated which in turn ionise the gas. An avalanche of charges is produced giving rise to and electric pulse on the anode wire.

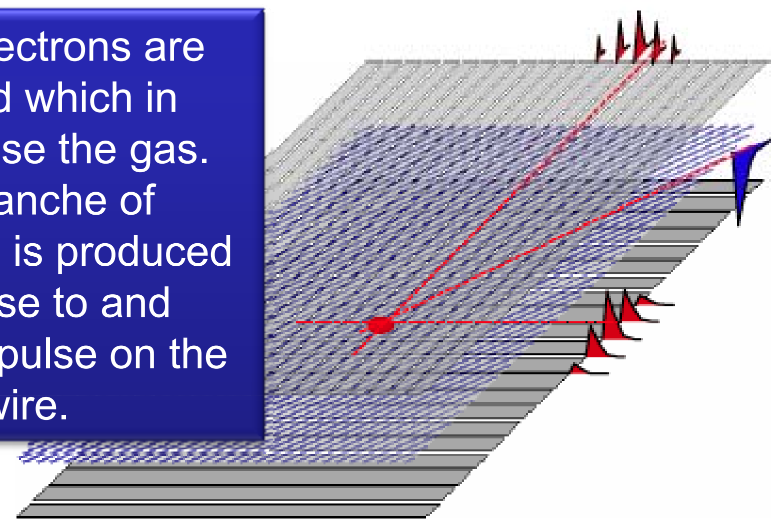

Centre of gravity

Types of Avalanches
Modes of Operation

Proportional region: A=10^3-10^4

Semi-proportional region: A=10^4-10^6

Saturation region: A > 10^8
(independent of the number of primary electrons)

Streamer region: A > 10^7
Avalanche along the particle track

Limited Geiger region: Avalanche propagated by UV photons

Geiger region: A = 10^8
Avalanche along the entire wire

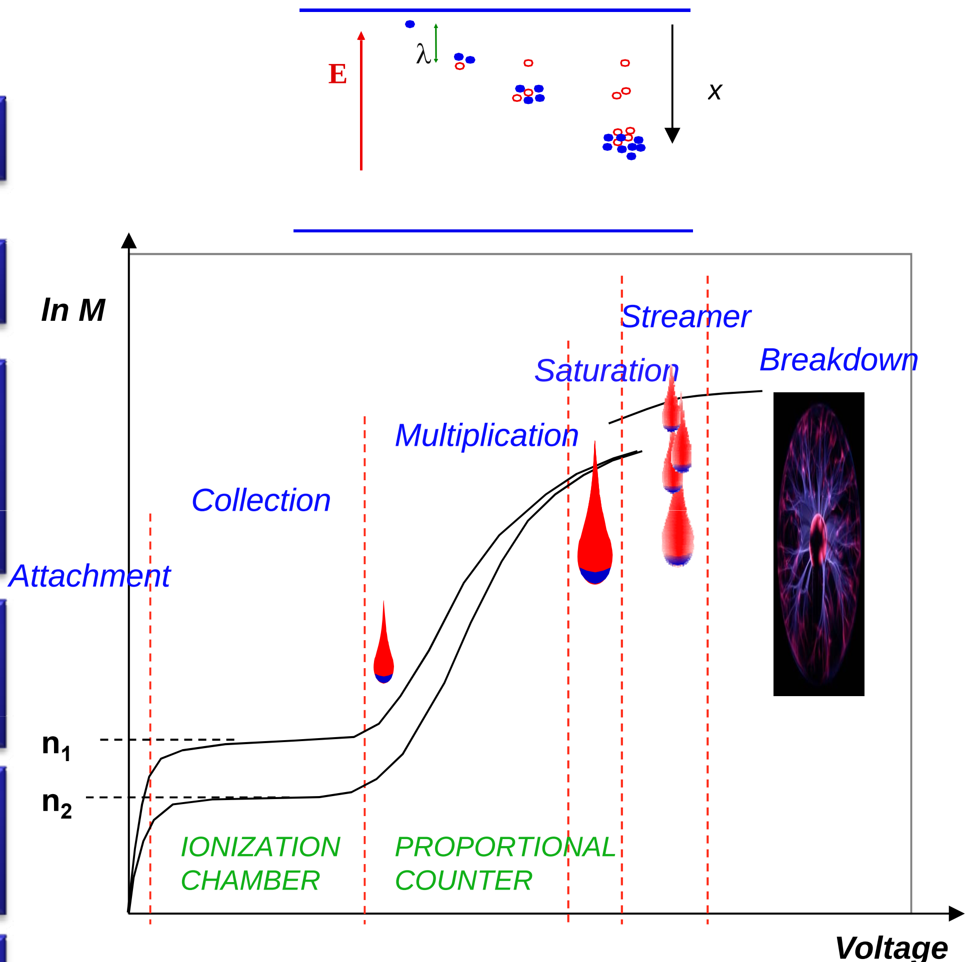

Requirements for Gas Mixtures

- Fast: an event must be unambiguously identified with its bunch crossing

  Leads to compromise between high drift velocity and large primary ionization statistics

- Drift velocity saturated or have small variations with electric and magnetic fields
- Well quenched with no secondary effects like photon feedback and field emission: stable gain well separated form electronics noise
- Fast ion mobility to inhibit space charge effects

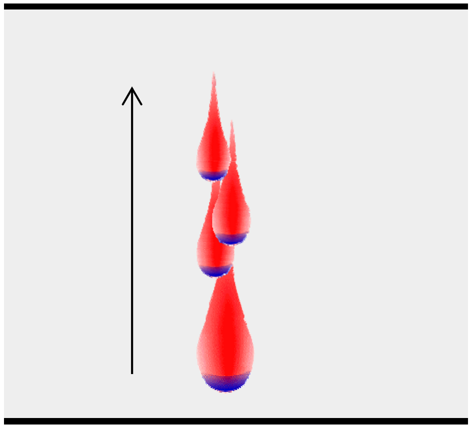

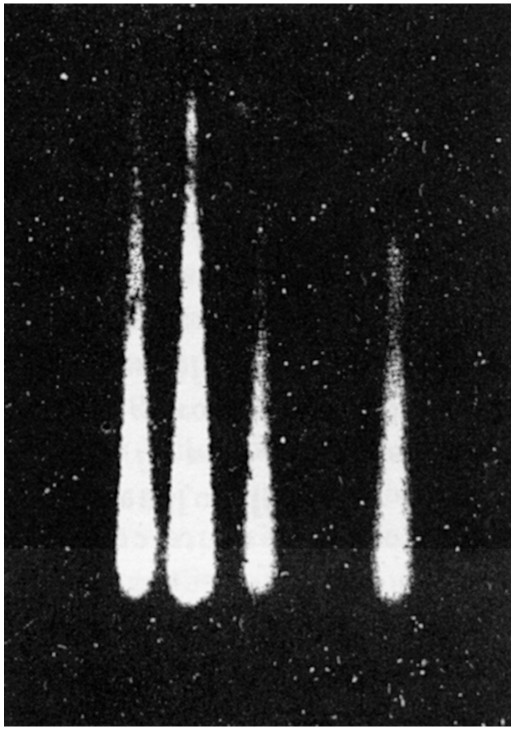

Properties of commonly used gases

An ionizing particles passing through a gas produces free electrons and ions in amounts that depend on the atomic number, density and ionization potential of the gas and energy and charge of the incident particle

N_p: number of primary electron pair per cm.
N_t: total number of electron ion pairs (from further ionization)

Gas	Z	A	Density 10^{-3} (g/cm^3)	E_x (eV)	E_i (eV)	w_i (eV)	$[dE/dx]_{mip}$ (keV cm^{-1})	n_p (cm^{-1}) N.T.P	n_t (cm^{-1}) N.T.P.	Radiation Length (m)
He	2	2	0.178	19.8	24.5	41	0.32	4.2	8	745
Ar	18	39.9	1.782	11.6	15.7	26	2.44	23	94	110
Ne	10	20.2	0.90	16.67	21.56	36.3	1.56	12	43	345
Xe	54	131.3	5.86	8.4	12.1	22	6.76	44	307	15
CF_4	42	88	3.93	12.5	15.9	54	7	51	100	92.4
DME	26	46	2.2	6.4	10.0	23.9	3.9	55	160	222
CO_2	22	44	1.98	5.2	13.7	33	3.01	35.5	91	183
CH_4	10	16	0.71	9.8	15.2	28	1.48	25	53	646
C_2H_6	18	30	1.34	8.7	11.7	27	1.15	41	111	340
$i\text{-}C_4H_{10}$	34	58	2.59	6.5	10.6	23	5.93	84	195	169

Requirements for Gas Mixtures

Noble Gases

Electrons moving in an electric field may still attain a steady distribution if the energy gain per mean free path << electron energy

Momentum transfer per collision is not constant.

Electrons near Ramsauer minimum have long mean free paths and therefore gain more energy before experiencing a collision.

Drift velocity depends on pressure, temperature and the presence of pollutants (e.g. water or oxygen)

Cross-section for electron collisions in Argon

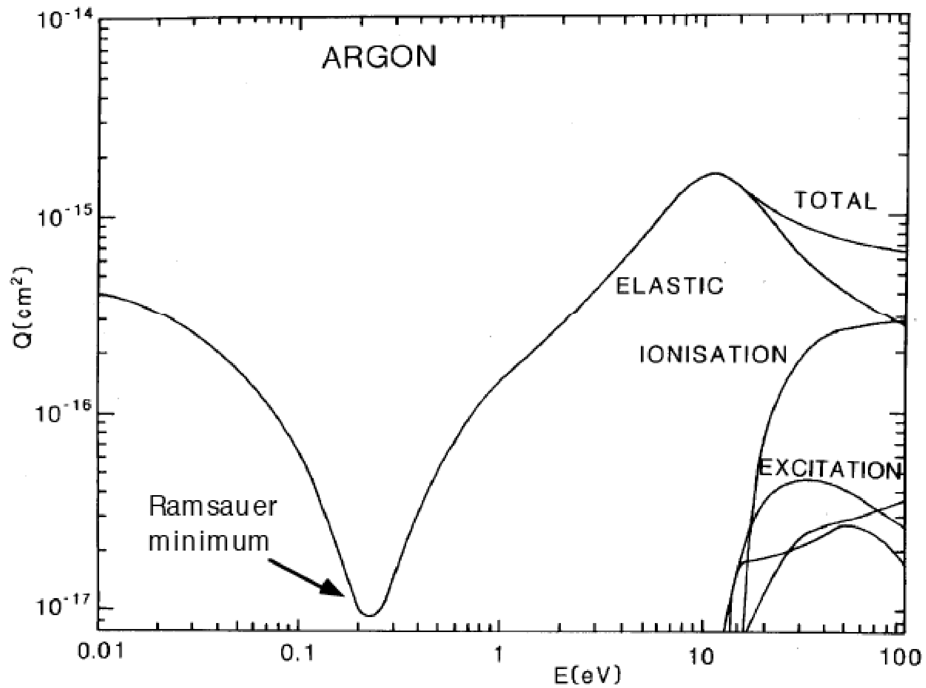

Requirements for Gas Mixtures

Poly-atomic gases

Poly-atomic molecular and organic gases have other modes of dissipating energy: molecular vibrations and rotations

In CO_2 vibrational collisions are produced at smaller energies (0.1 to 1 eV) than excitation or ionization

Vibrational and rotational cross-sections results in large mean fractional energy loss and low mean electron energy

Electron collision cross-sections for CO_2

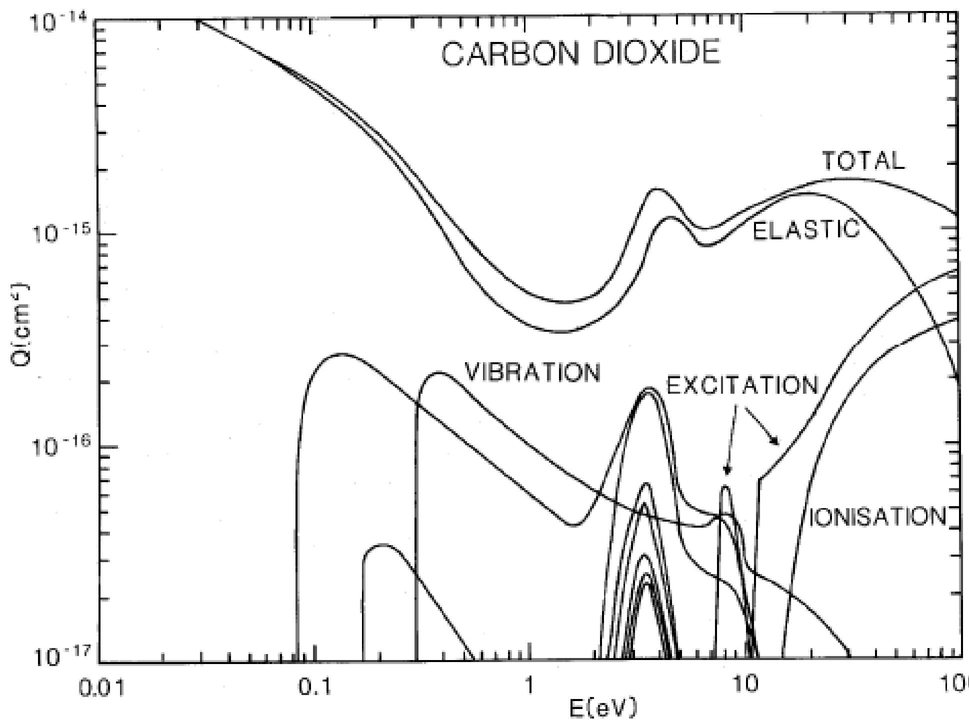

Mean or 'characteristic electron energy' represents the average 'temperature' of drifting electrons

Requirements for Gas Mixtures

Pollutants

Pollutants modify the transport parameters and electron loss occurs (capture by electro-negative pollutants)

The static electric dipole moment of water increases inelastic cross-section for low energy electrons thus dramatically reducing the drift velocity

Electron capture phenomenon has a non negligible electron detachment probability

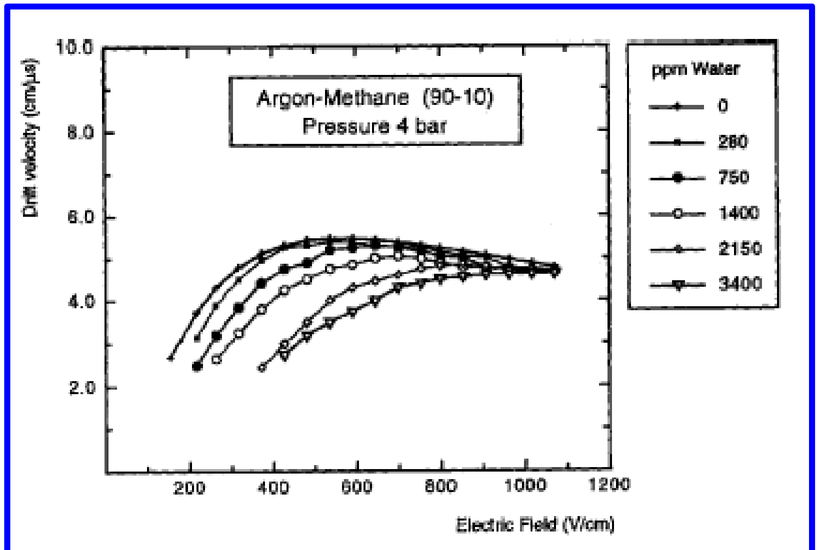

Mean electron capture length

Gas Mixture	Electric Field [V/cm]	lp[cm]
Ar-CH_4 (90-10)	150	5.1 10^{-2}
Ar-CH_4 (90-10)	250	3.4 10^{-2}
Ar-CH_4 (80-20)	100	1.6 10^{-2}
Ar-CH_4 (80-20)	200	2.9 10^{-2}
Ar-CO_2 (80-20)		9.3 10^{-2}
Xe-CH_4 (90-10)	~ 500	7.8 10^{-2}

Transport Properties of Gas Mixtures

ELECTRIC FIELD E = 0: THERMAL DIFFUSION

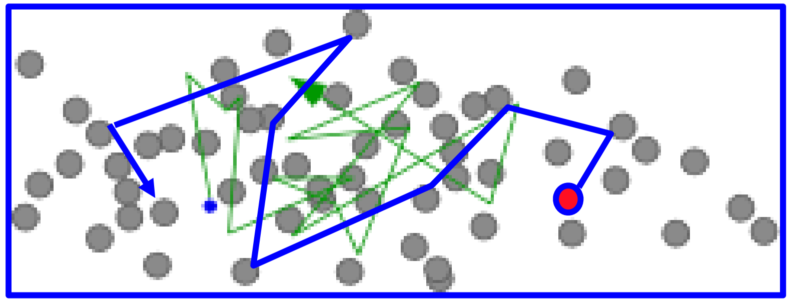

ELECTRIC FIELD E > 0: CHARGE TRANSPORT AND DIFFUSION

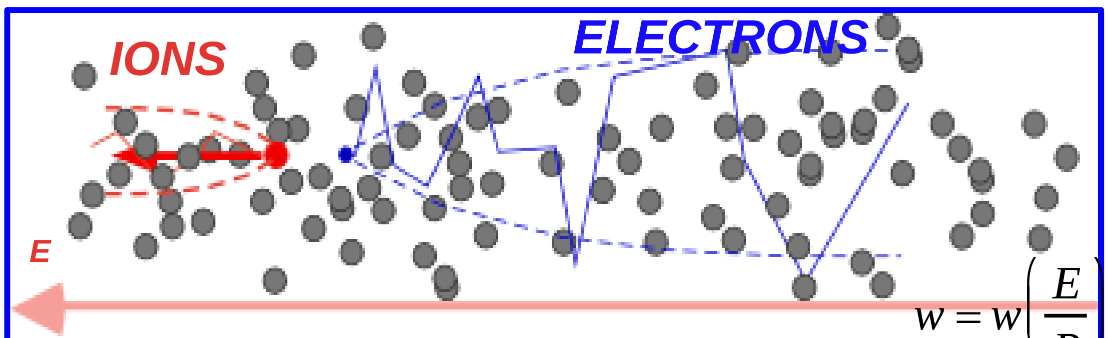

$$w = w\left(\frac{E}{P}\right)$$

Drift velocity and diffusion are gas and field dependent:

$$D = g\left(\frac{E}{P}\right) \qquad \sigma = \frac{1}{\sqrt{P}} F\left(\frac{E}{P}\right)$$

Transport Properties of Gas Mixtures

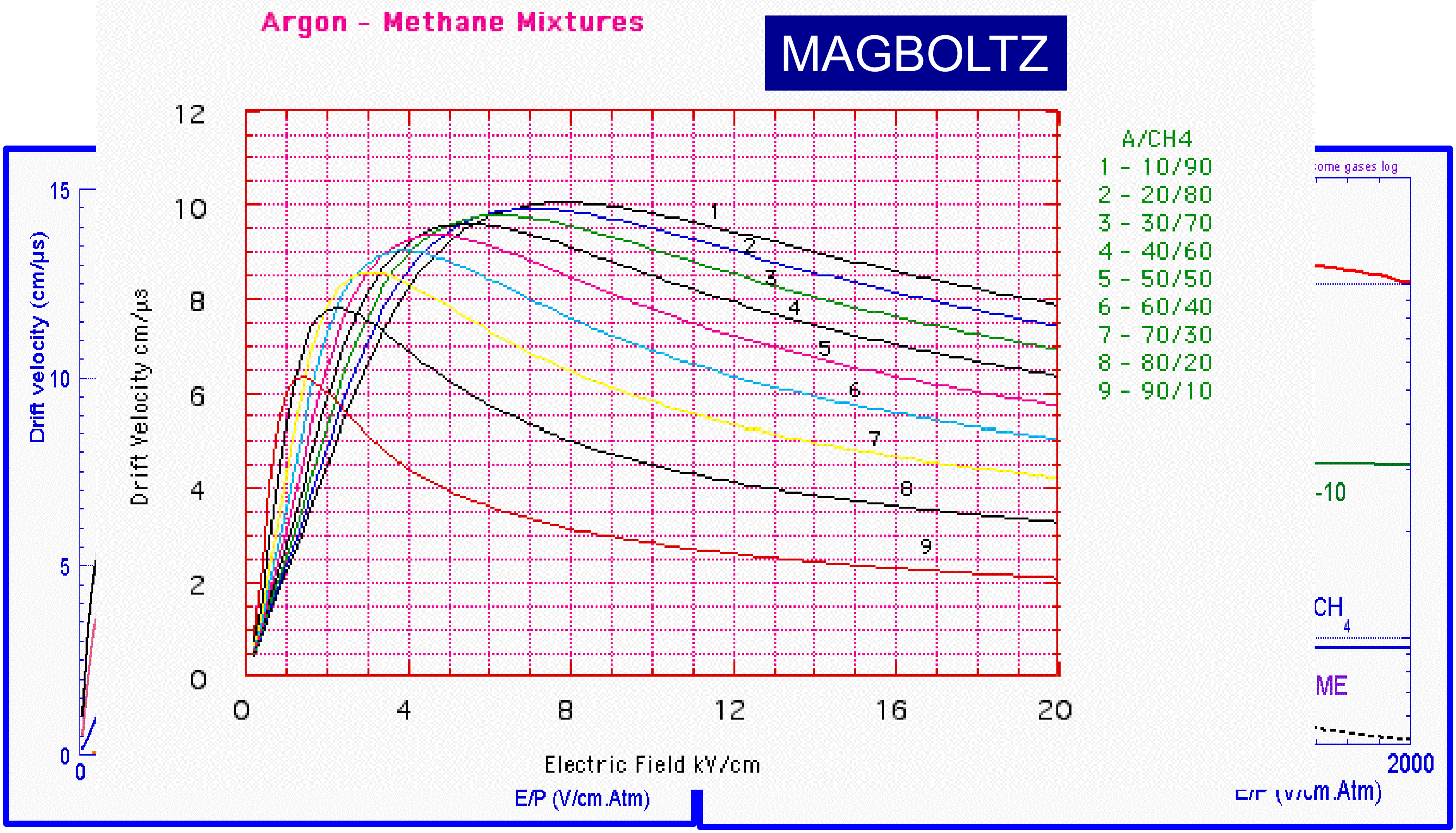

Transport Properties of Gas Mixtures

Lorentz Angle

Reduction in B Field

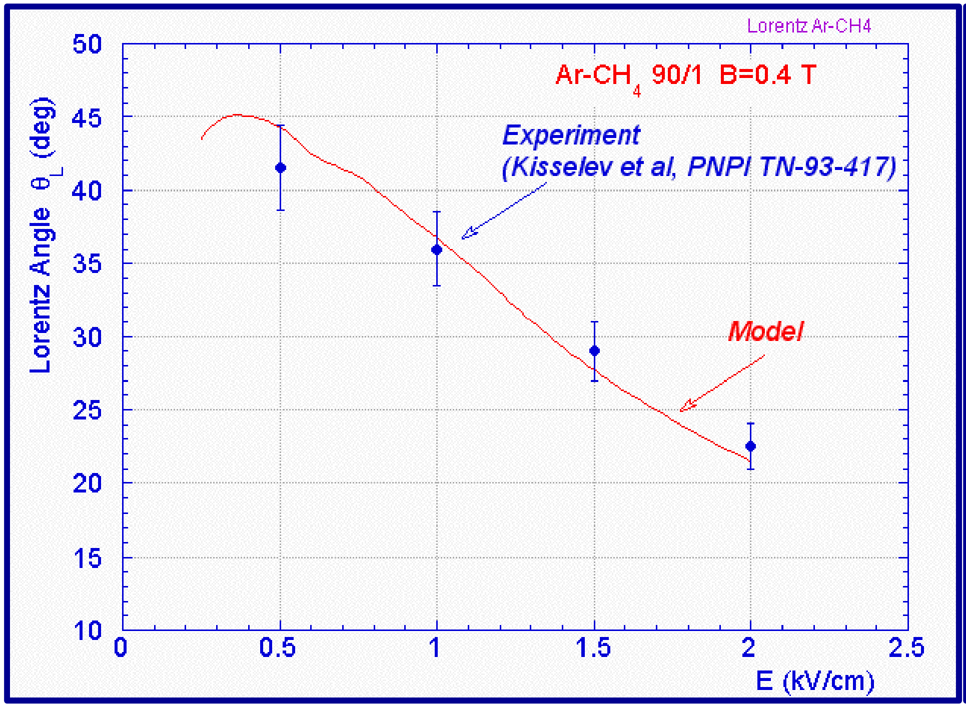

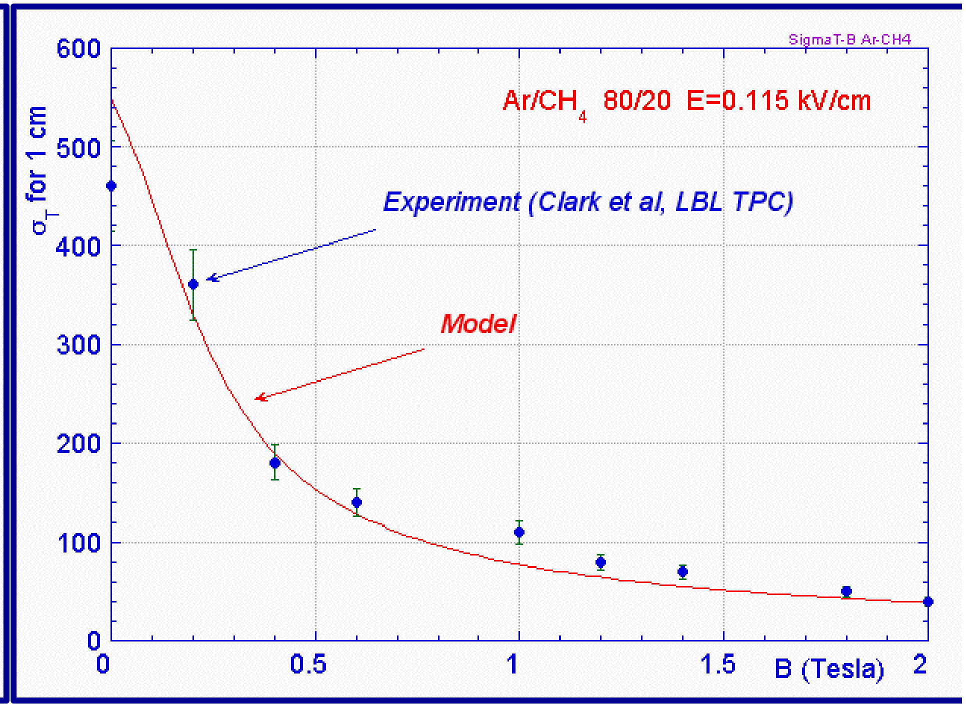

Ion Mobility

Ions drift slowly because of their large mass and scattering cross-section. Similar spectrum to the Maxwell energy distribution of the gas molecules.

Average drift velocity (W+) increases with the field strength (E) and decreases as the gas pressure, P, increases.

A pressure increase leads to a shorter mean free path (distance during which an ion is accelerated before losing its energy in a collision).

The ion mobility, μ^+, defined as $\mu^+=W^+(P/E)$, is constant for a given ion type in a given gas.

Gas	Ion	Mobility ($cm^2\ V^{-1}\ s^{-1}$)
He	He^+	10.4
Ne	Ne^+	4.7
Ar	Ar^+	1.54
Ar	CH_4^+	1.87
Ar	CO_2^+	1.72
CH_4	CH_4^+	2.26
CO_2	CO_2^+	1.09

Signal Development
Parallel Plate Chamber

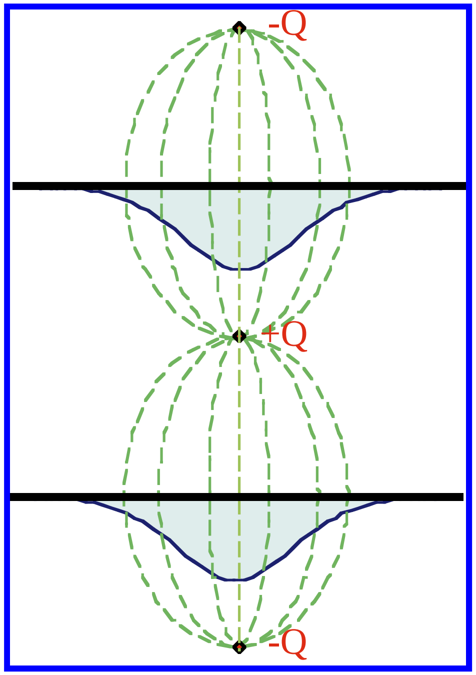

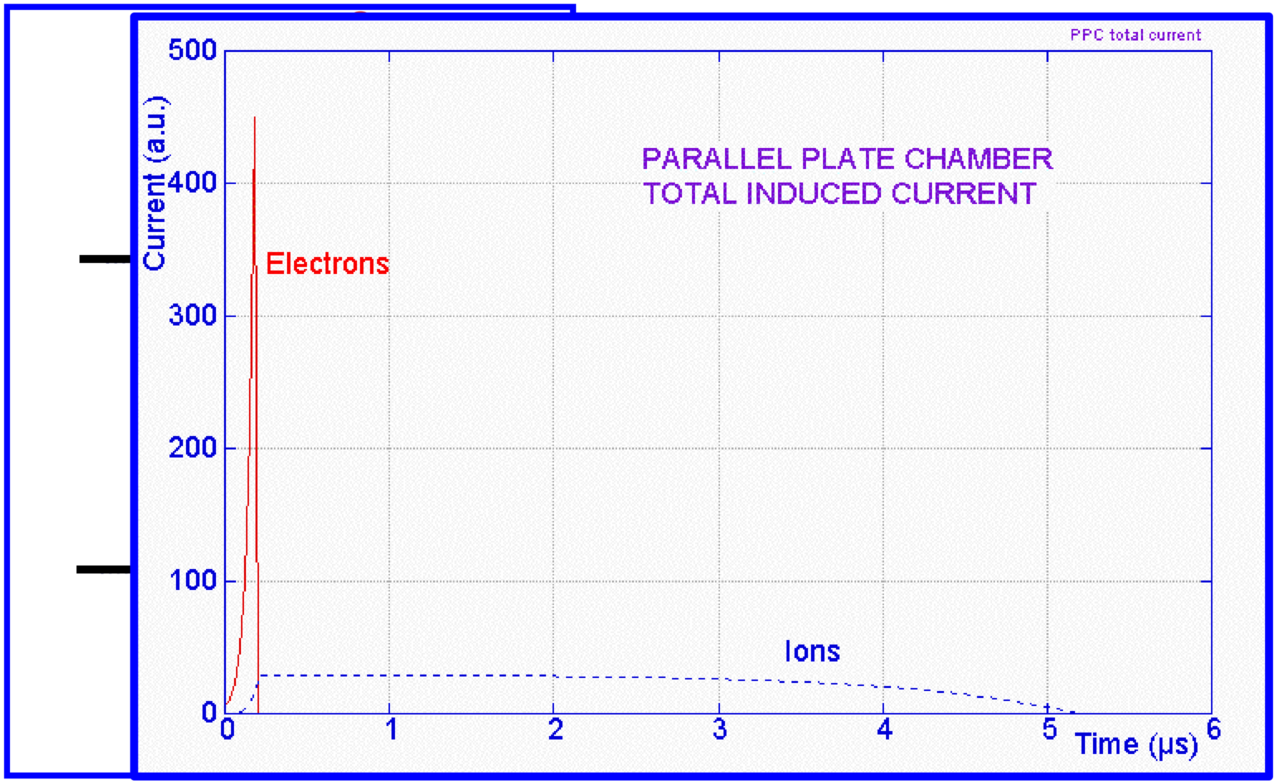

A charge +Q between two conductors induces two negative charge profiles (image charge)

Moving the charge modifies the induced charge profile on the conductors and generates detectable signals

+Q towards an electrode: positive induced signal

Induced signals are equal and opposite on anode and cathode

RESISTIVE
PLATE
CHAMBERs

Resistive Plate Chambers

Place resistive plates (Bakelite or window glass) in front of the metal electrodes

↓

Sparks cannot develop because the resistivity and capacitance will allow only a very localized discharge.

↓

Large area detectors can be made

Rate limit of ~ kHz/cm^2

CMS RPCs

AVALANCHE MODE

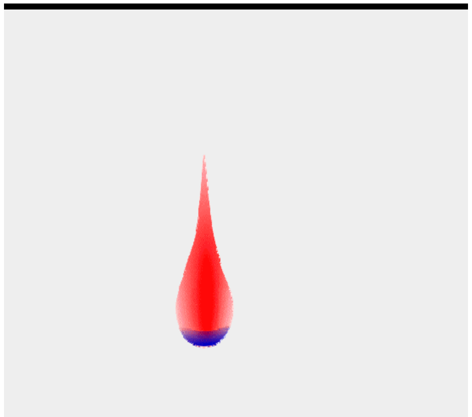

TRANSITION AVALANCHE TO STREAMER

PHOTON MEDIATED BACKWARD PROPAGATION:
STREAMER   NB GAS MIXTURE !

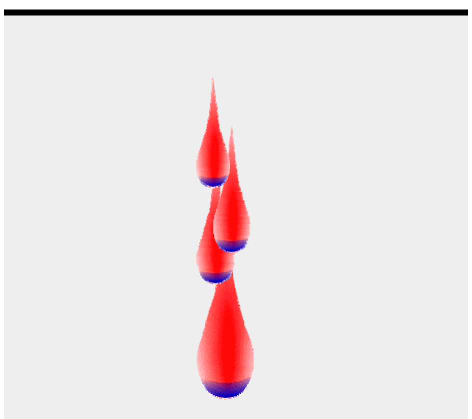

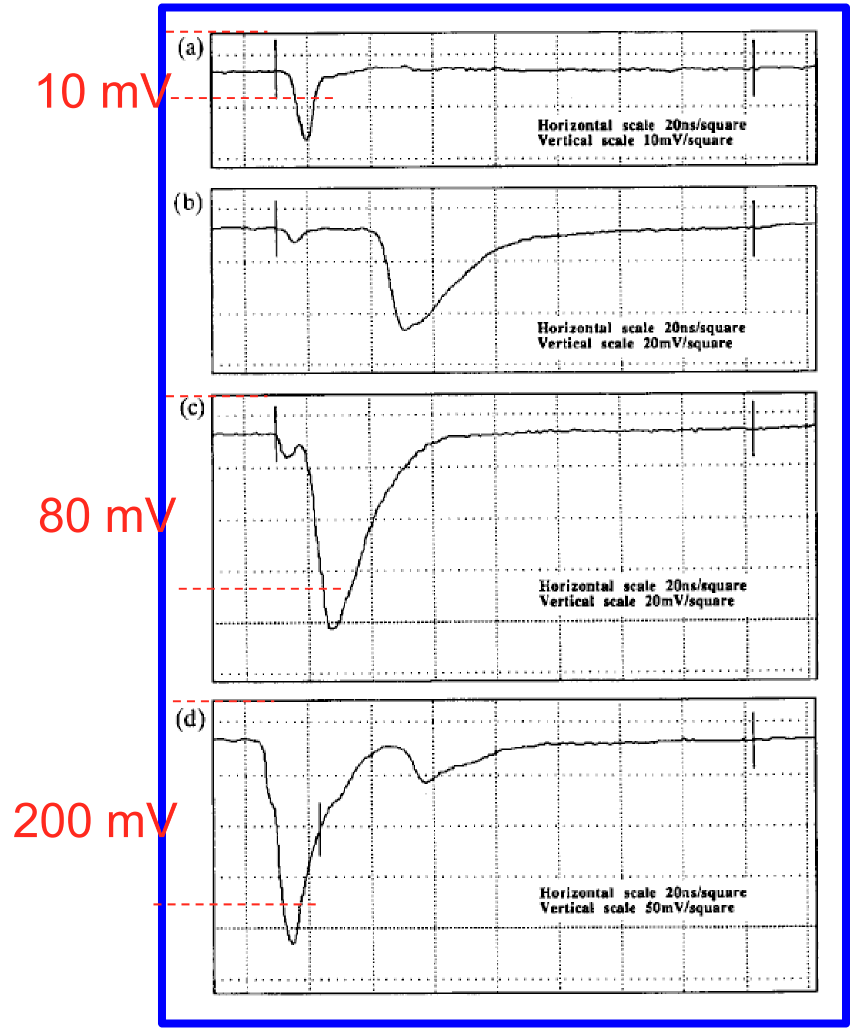

R. Cardarelli, V. Makeev, R. Santonico, Nucl. Instr. and Meth. A382(1996)470

RPC RATE CAPABILITY: AVALANCHE VS STREAMER OPERATION

STREAMER MODE:

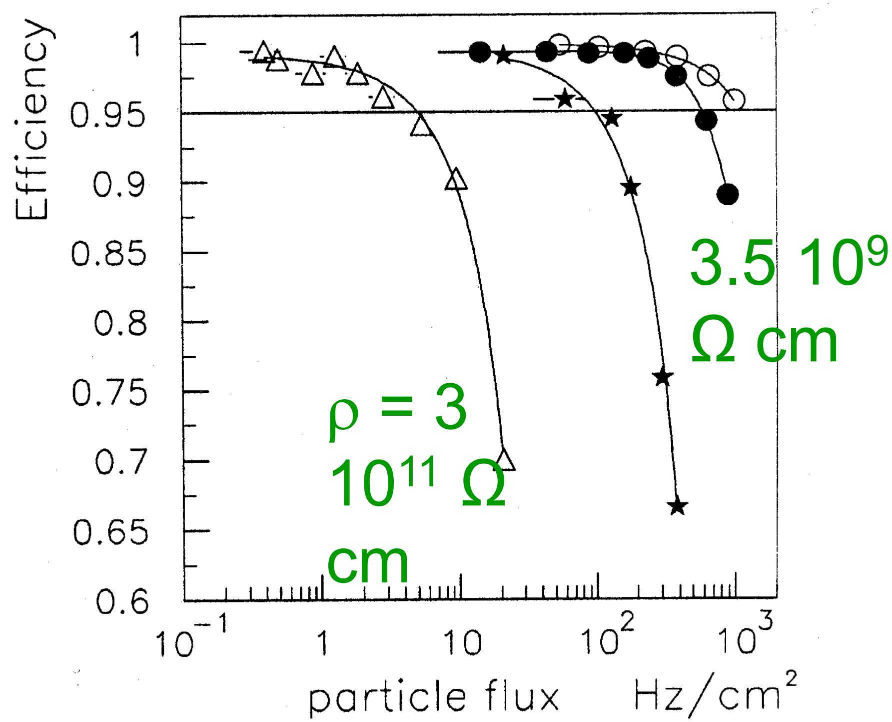

AVALANCHE

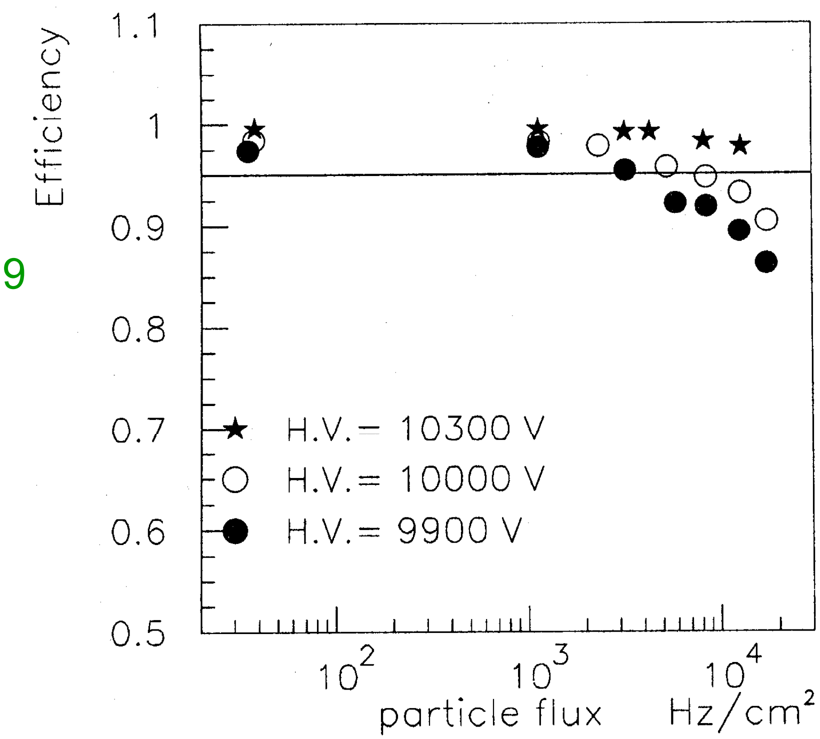

R. Arnaldi et al, Nucl. Physics B (Suppl) 78 (1999) 84

RPC RATE CAPABILITY:

DEPENDS ON GAIN AND
ELECTRODES RESISTIVITY

MATERIAL	VOLUME RESISTIVITY (Ω.cm)
Pestov glass	10^{9}-10^{10}
Phenolic (Bakelite)	10^{10}-10^{11}
Cellulose	5.10^{12}
Borosilicate glass	10^{13}
Melamine	2.10^{13}

PROPORTIONAL (AVALANCHE) OPERATION:

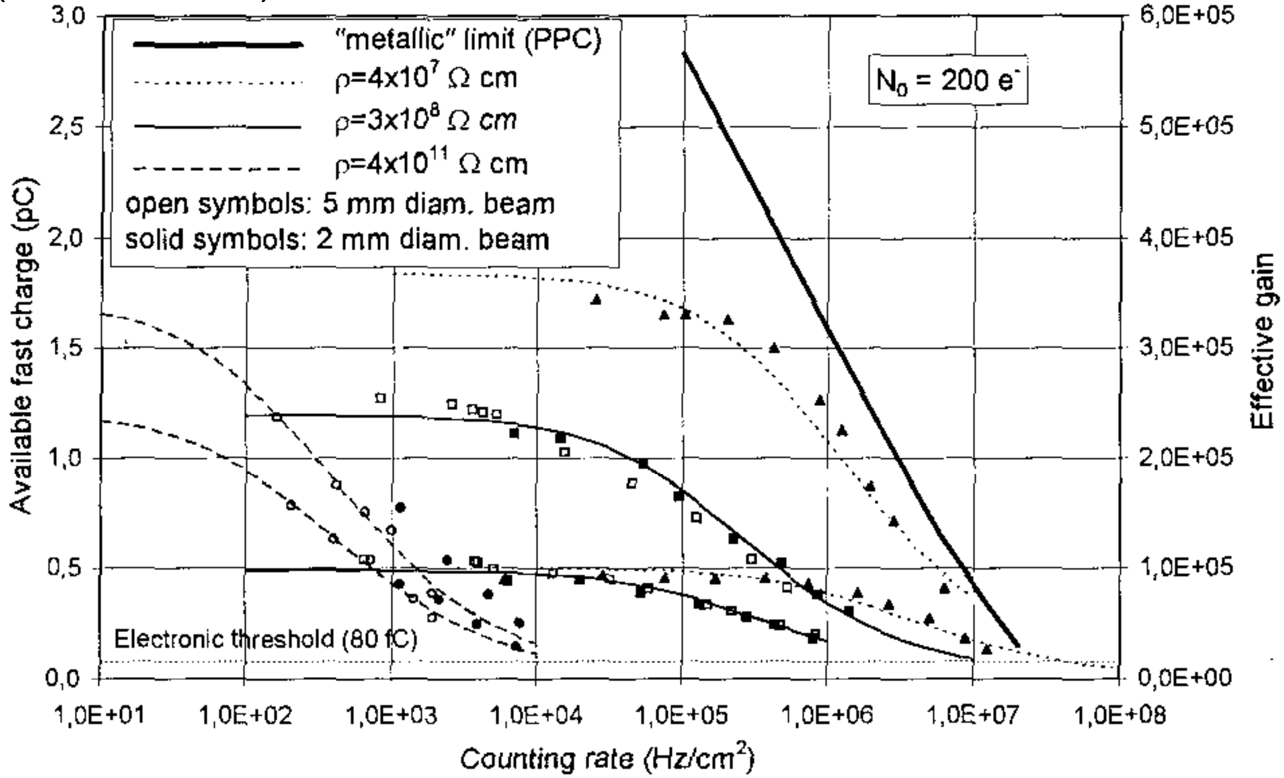

P. Fonte, Scientifica Acta XIII N2(1997)11

GAP DEPENDENCE

THE SEPARATION AVALANCHE-STREAMER DEPENDS ON THE GAP:

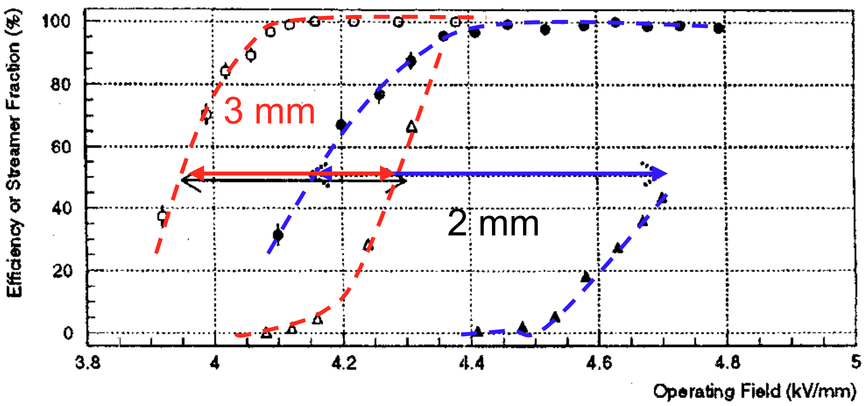

○ 3 mm EFFICIENCY (Threshold = 30 mV)

△ 3 mm STREAMER FRACTION

● 2 mm EFFICIENCY (Threshold = 30 mV)

▲ 2 mm STREAMER FRACTION

R. Santonico, Scient. Acta XII N2(1997)1

SMALL ADDITIONS OF ELECTRO-NEGATIVE GASES EXTEND THE SEPARATION:

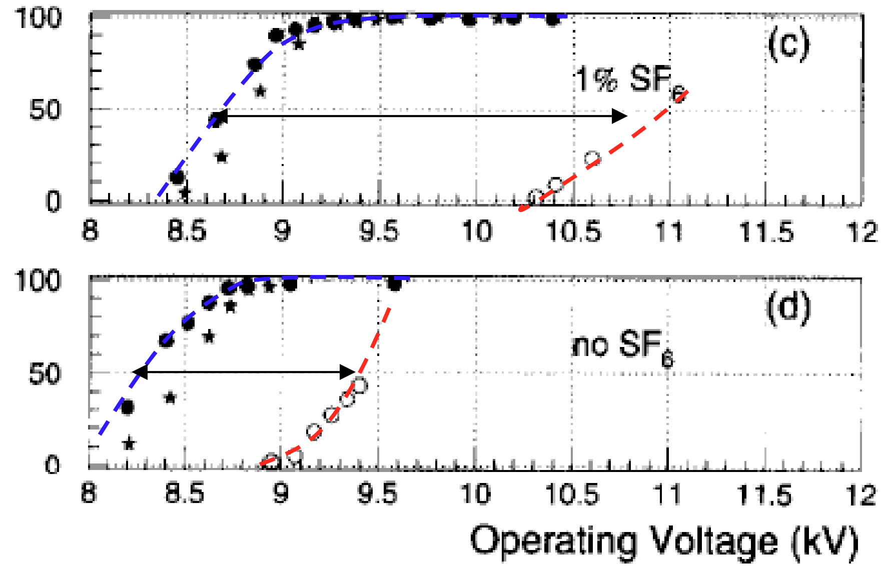

● EFFICIENCY (threshold = 30 mV)

★ EFFICIENCY (threshold = 100 mV)

○ STREAMER FRACTION

P. Camarri et al, Nucl. Instr. and Meth. A414(1998)317

Resistive Plate Chambers at LHC

FROM Panel discussion – RPC2012 Sharma and Diego Gonzalez

Classic RPCs

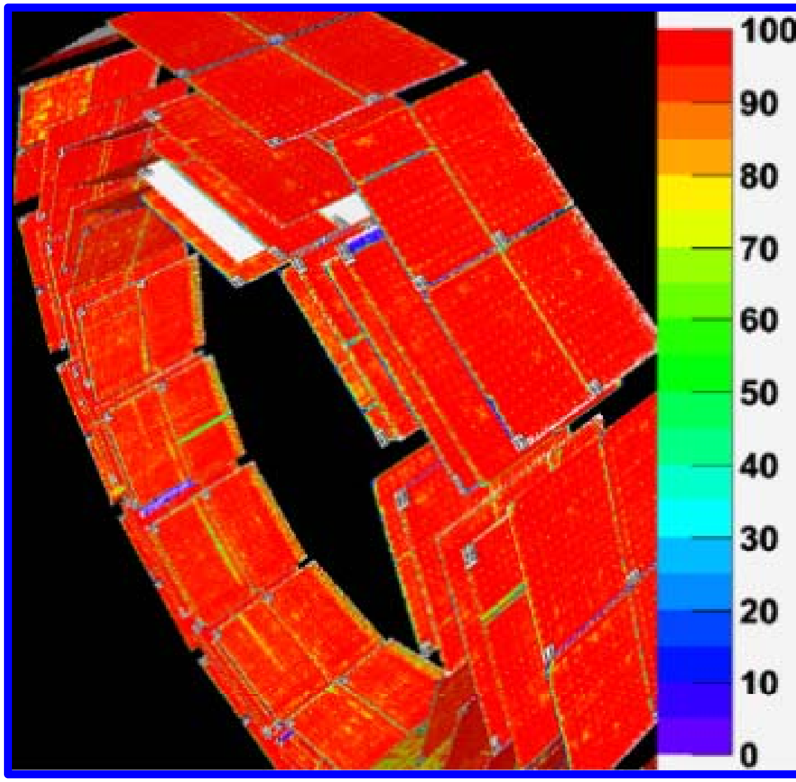

Multi-gap RPCs

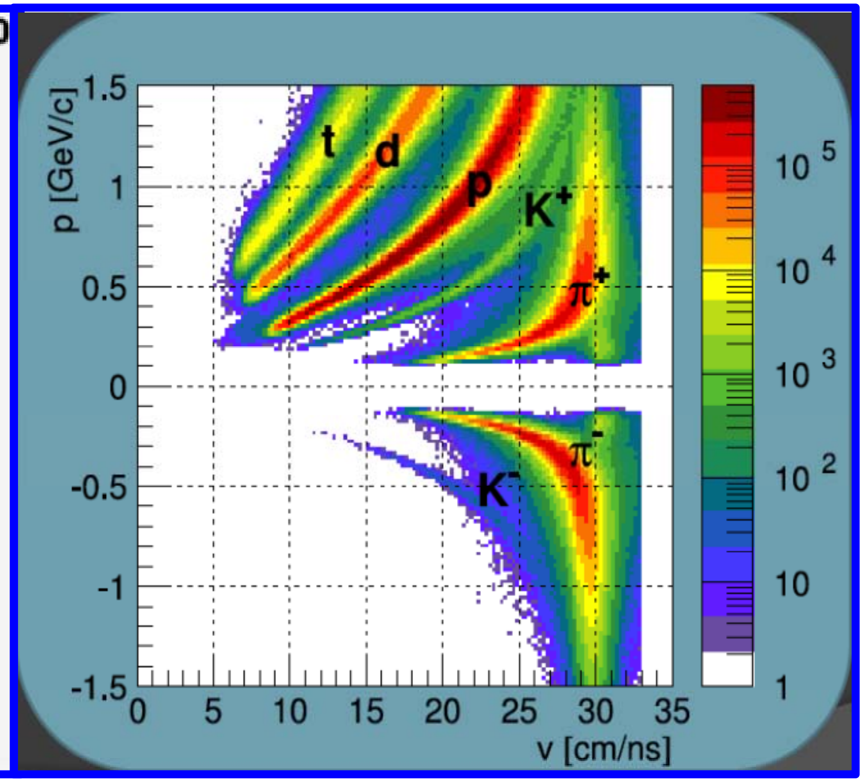

Left: Five radial layers of the classic RPCs constituting the CMS barrel wheel, with efficiency indicated on the right axis.

Right: particle identification from FOPI, using multi-gap timing RPCs. The plot is compatible with **a system resolution σ_T=90ps**

ONLY AT LHC 15, 000 m^2

Resistive Plate Chambers-Open Issues

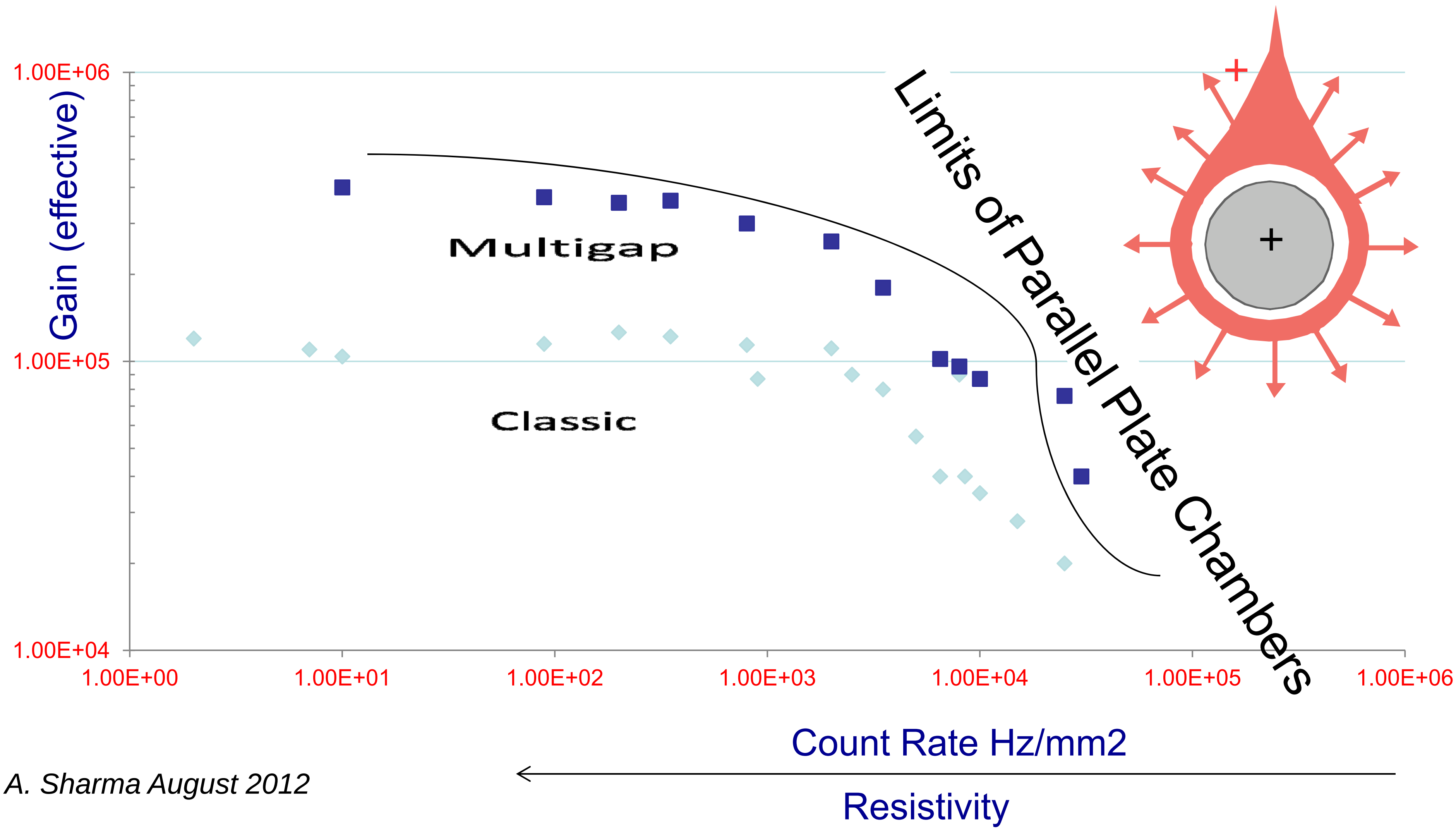

A. Sharma August 2012

Multiwire Proportional Chamber and derivatives

Cathode Strip Chambers CSC

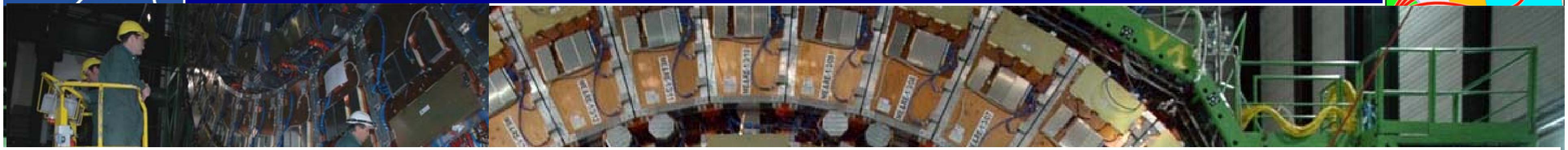

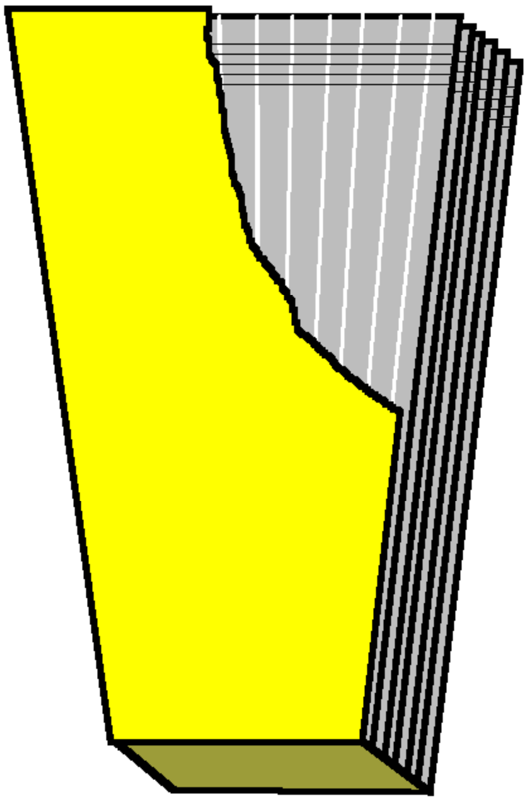

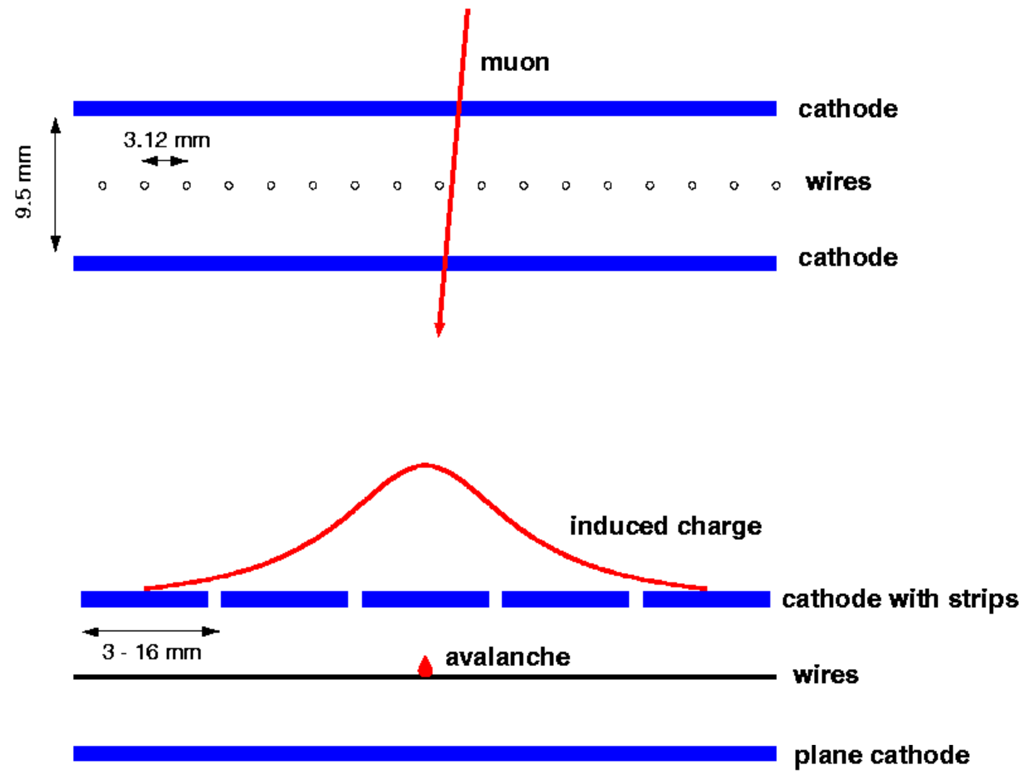

Drift Chambers

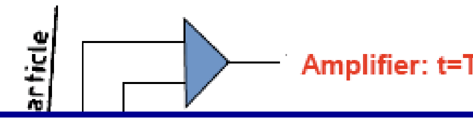

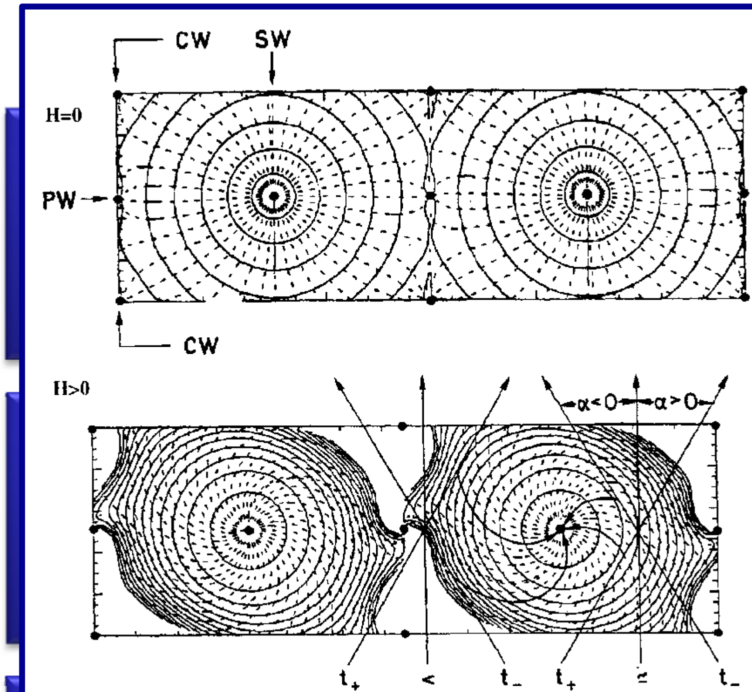

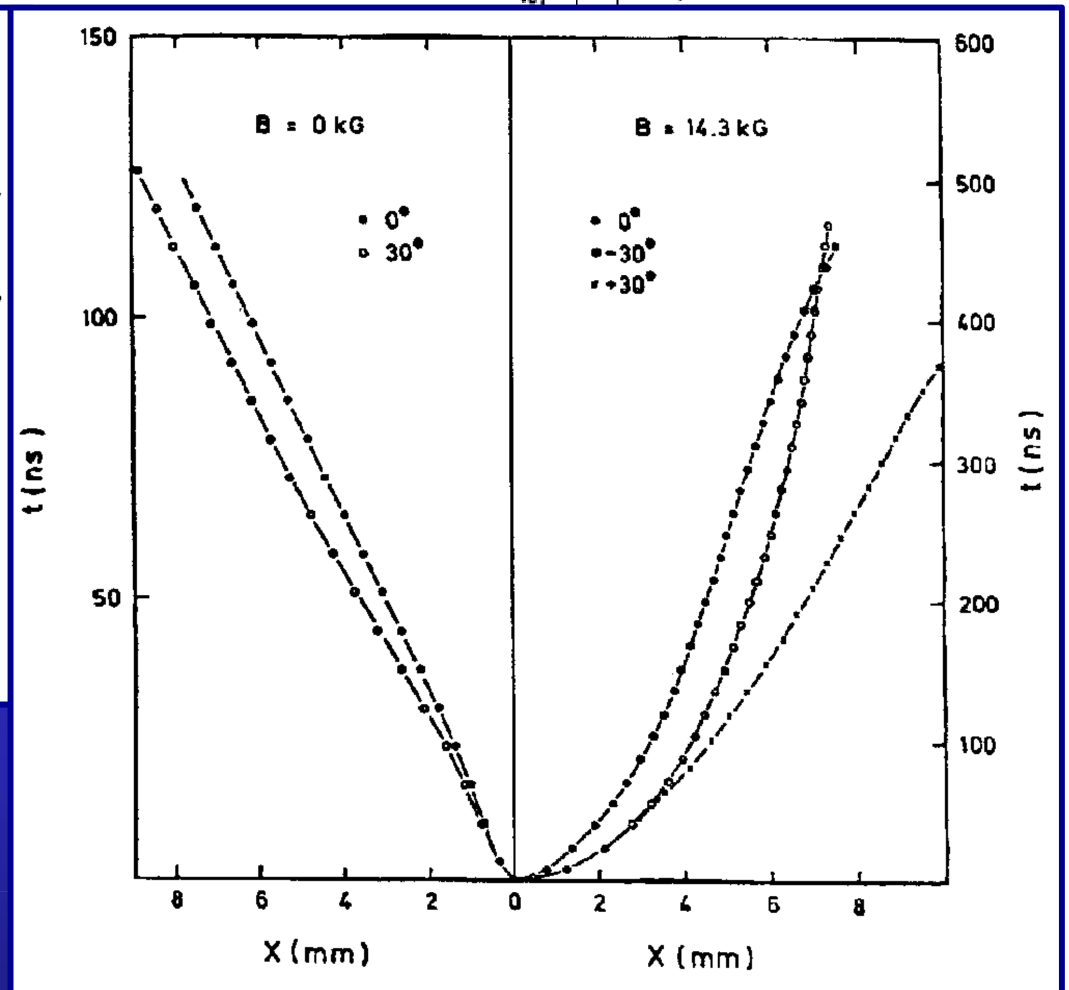

The time between the passage of the particle and the arrival of the electrons is measured → measure of the particles position. Can increase the wire distance to save electronics channels.

Time Projection Chamber (TPC)

A TPC is a gas-filled cylindrical chambers (with parallel E and B field) with MWPCs as endplates.

- Drift fields of 100-400 V/cm
- Drift times 10 - 100 μs
- Distance up to 2.5 m

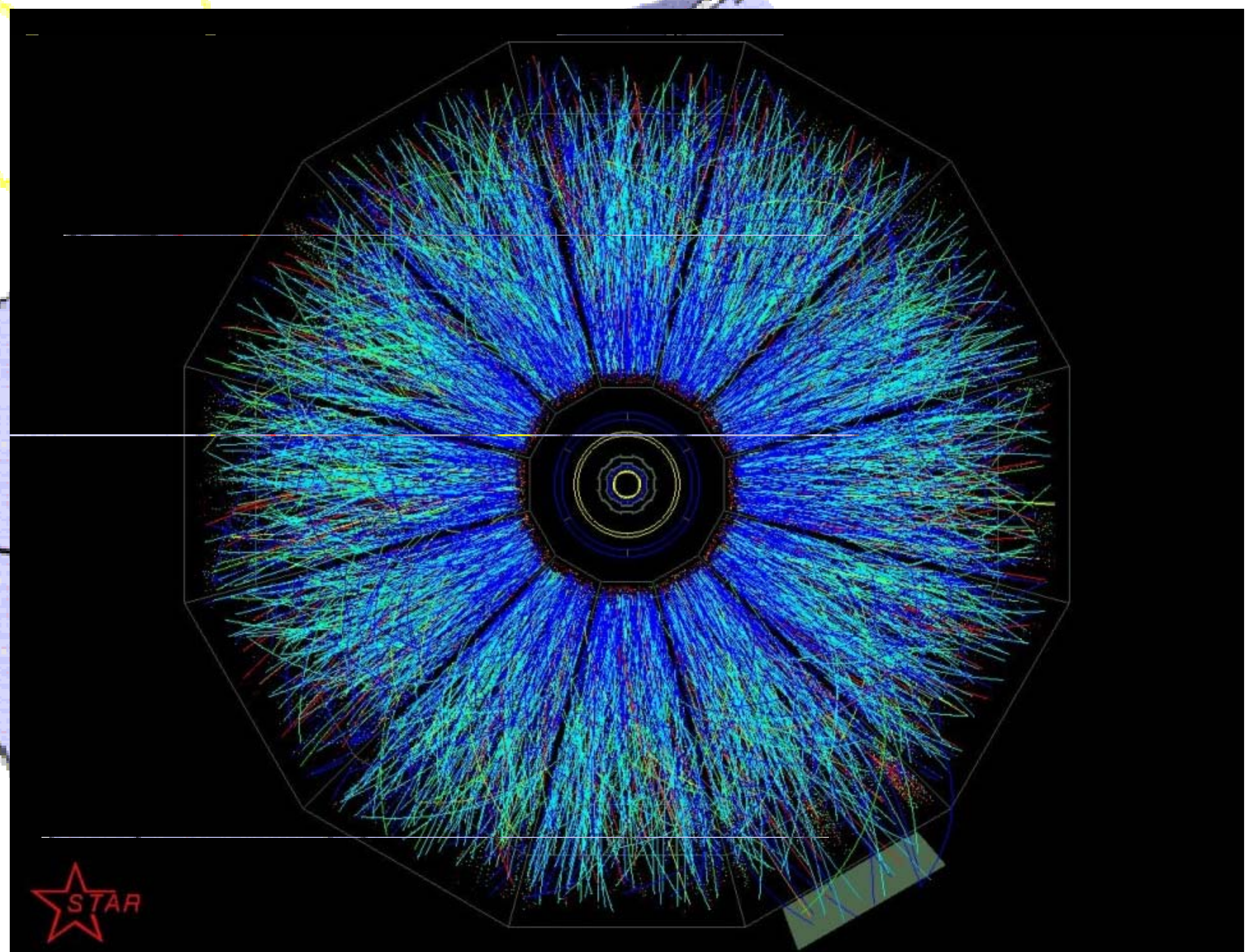

events.

Modern TPCs

STAR TPC

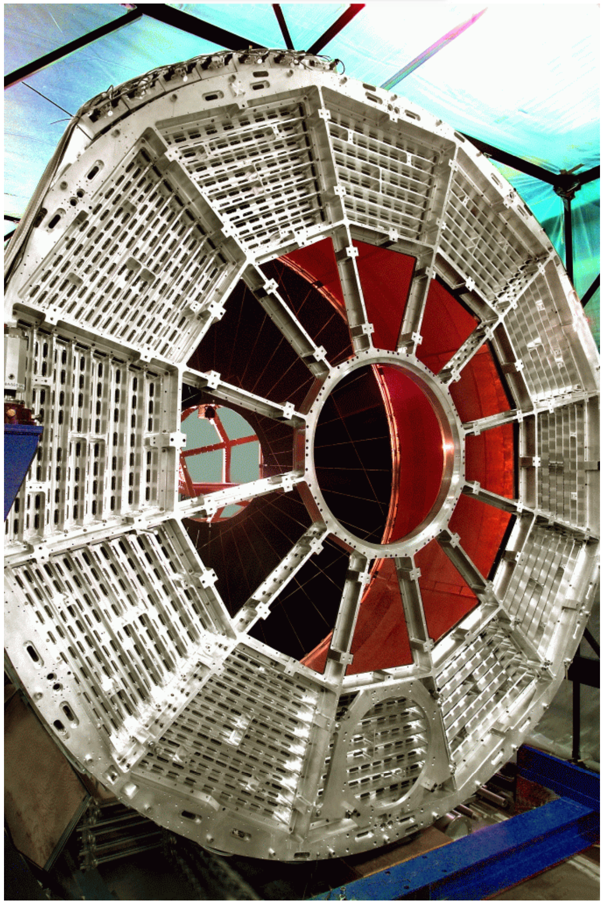

ALICE TPC

Energy-loss measurements

The Bethe Bloch Formula tool for Particle Identification

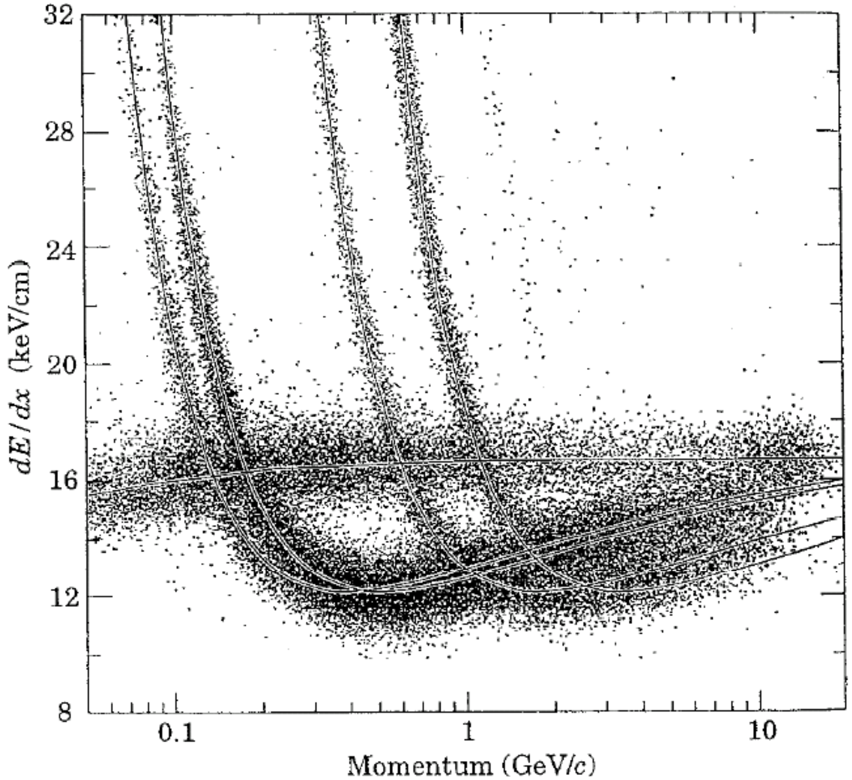

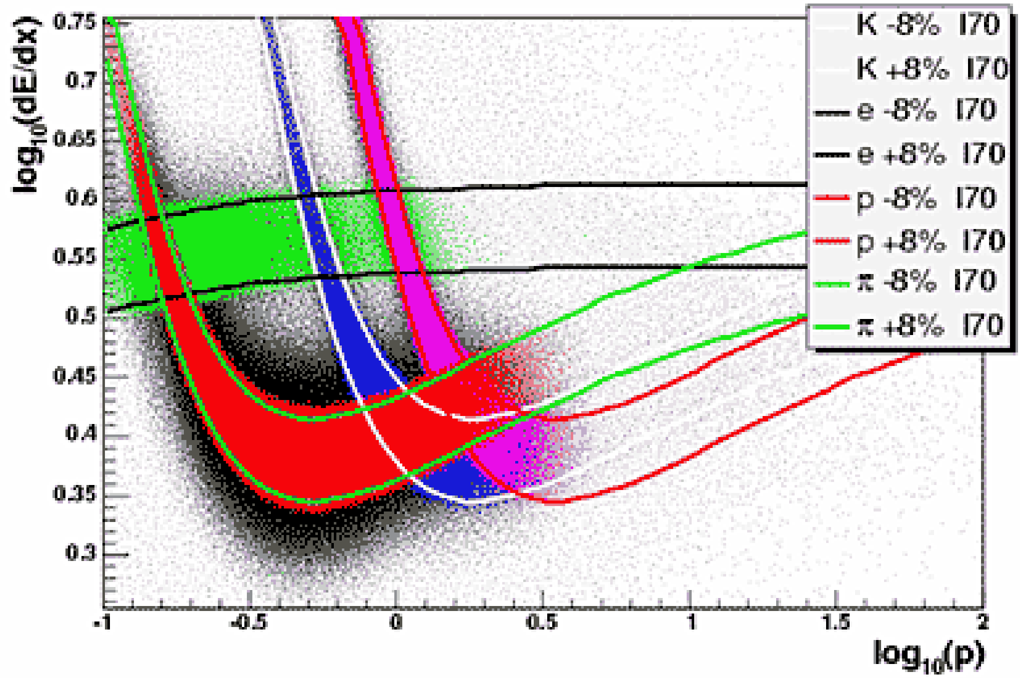

LIMITATIONS OF MULTIWIRE CHAMBERS

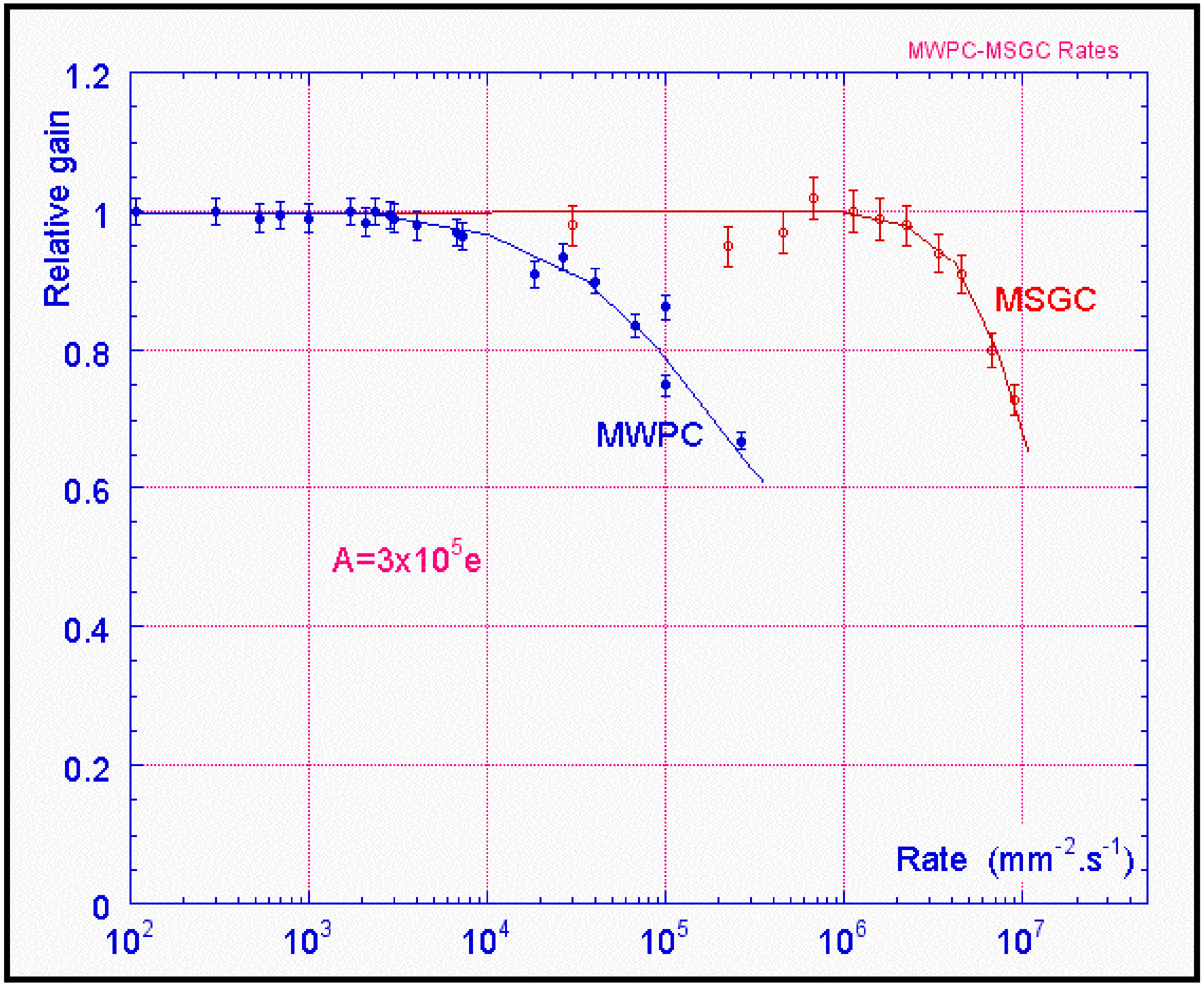

RATE CAPABILITY > 10^6/mm^2 s
SPACE ACCURACY ~ 40 μm rms
2-TRACK RESOLUTION ~ 400 μm

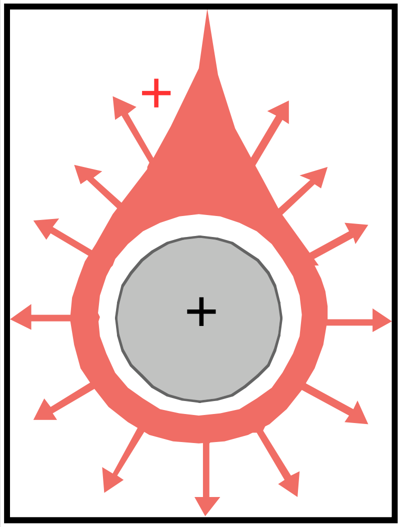

Micro Strip Generation

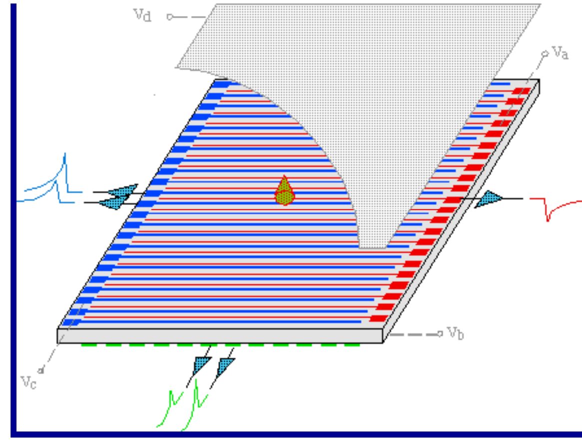

Micro-Strip Gas Chamber (MSGC) invented by Oed in 1988.

A pattern of thin anodes and cathode strips on a insulating substrate with a pitch of a few hundred μm.

Electric field from a drift electrode above and appropriate potentials applied.

Field Configuration in an MSGC

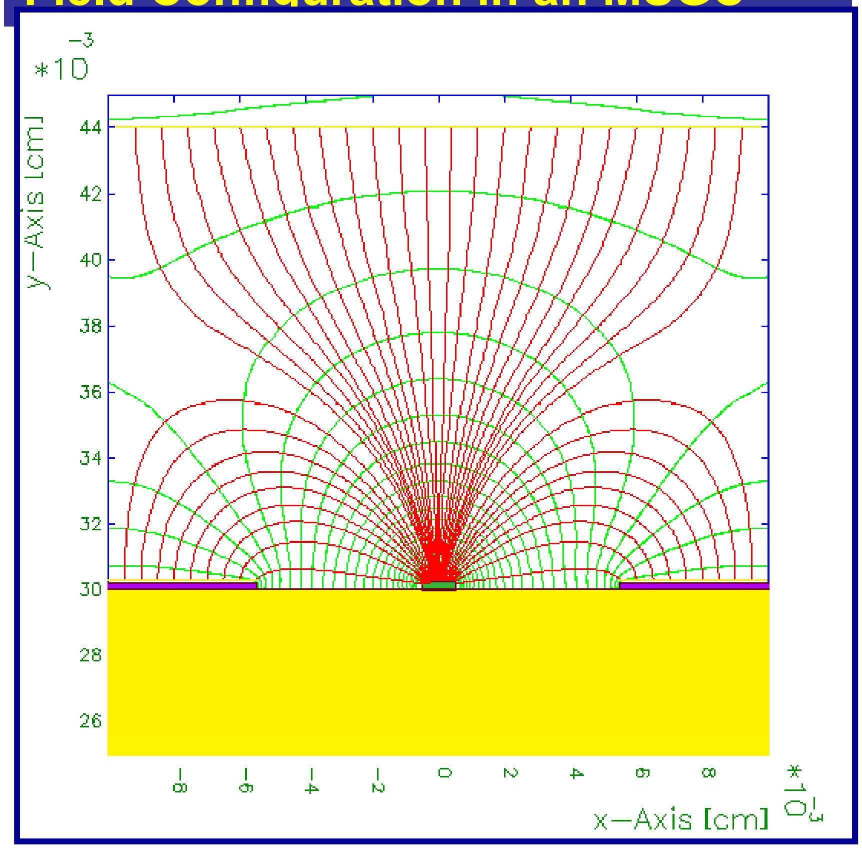

MSGC: DISCHARGE MECHANISMS

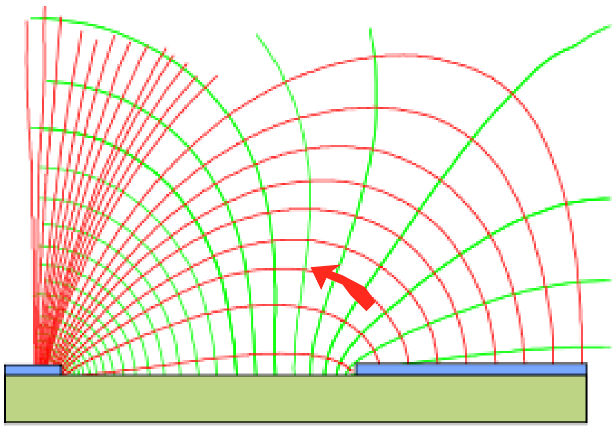

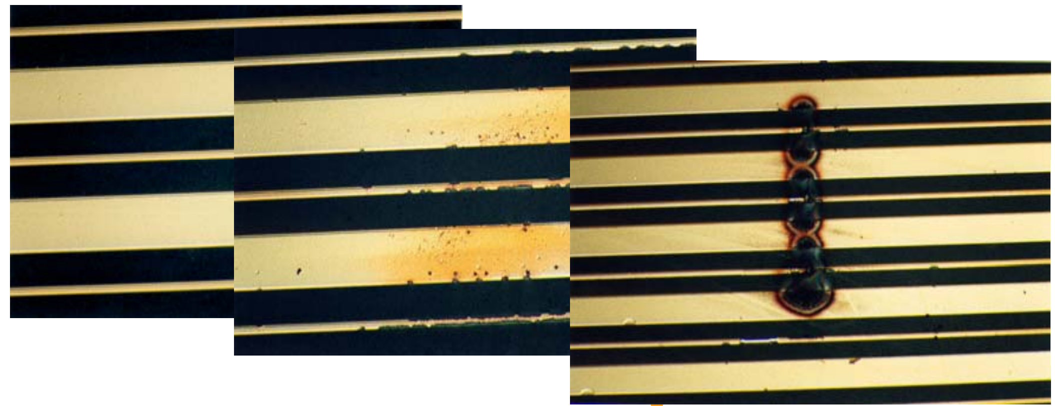

FIELD EMISSION FROM CATHODE EDGE

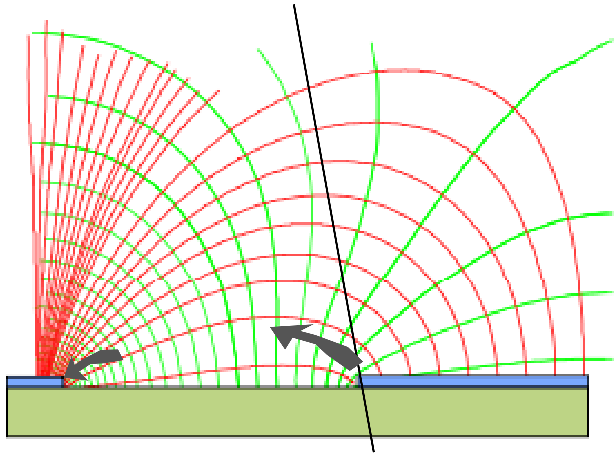

CHARGE PRE-AMPLIFICATION FOR IONIZATION RELEASED IN HIGH FIELD CLOSE TO CATHODE

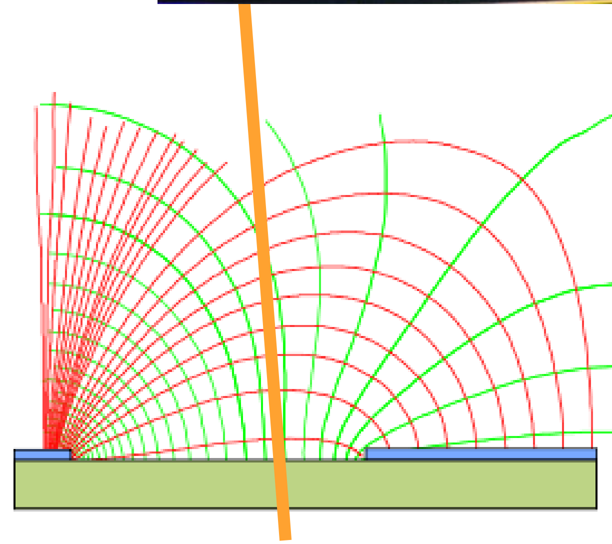

VERY HIGH IONIZATION RELEASE:
AVALANCHE SIZE EXCEEDS RAETHER'S LIMIT
$Q \sim 10^7$

Micropattern Era…

Microneedle Concept (1976)

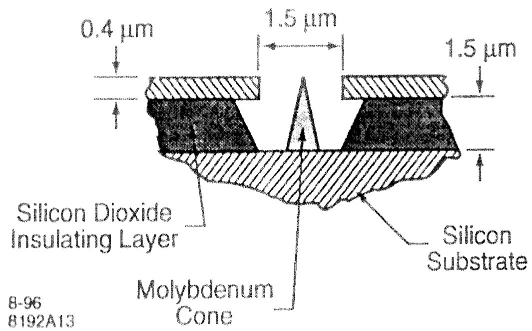

No observable gas gain due to fine needles (<<1µm) and small amplification region

Microdot Chamber Schematic (1996)

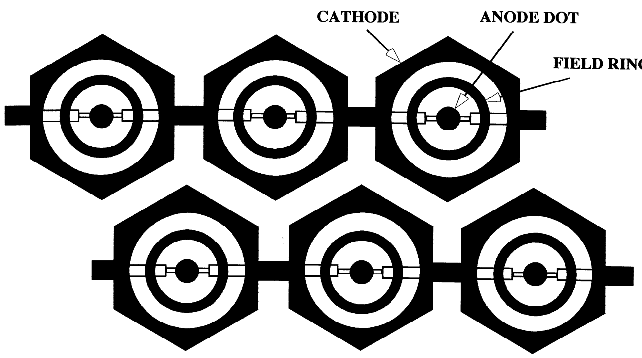

Ultimate gaseous pixel device with anode dotes surrounded by cathode rings. Very high gains (~10^6). Does not discharge up to very high gains.

Micro-Megas

Charpak and Giomataris 1996

Very asymmetric parallel plate chamber. Uses the semi-saturation of the Townsend coefficient at high fields (100kV/cm) in several gas mixtures, to ensure stability in operation with mips.

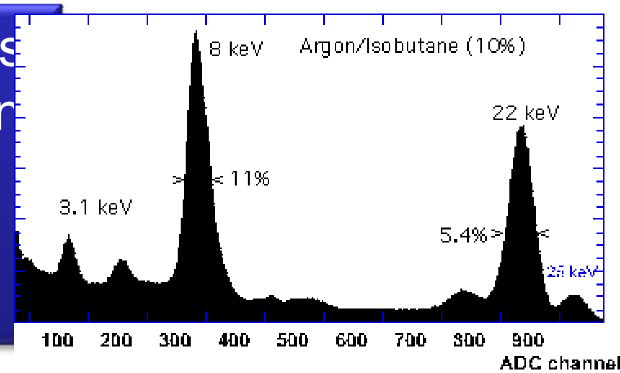

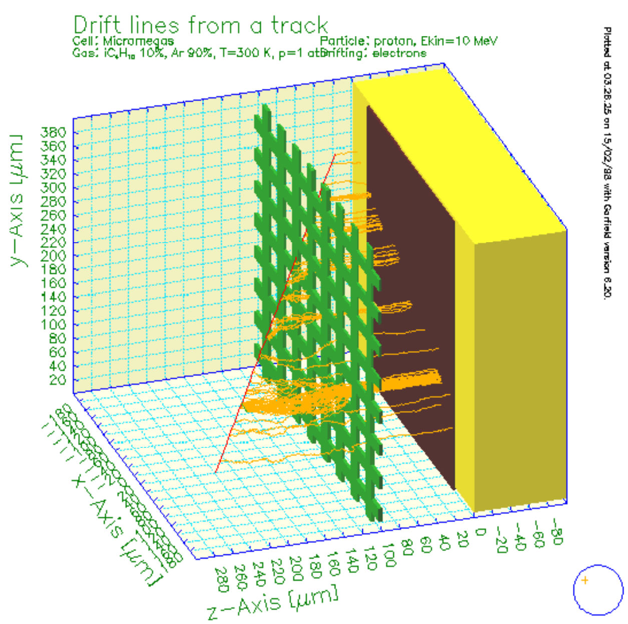

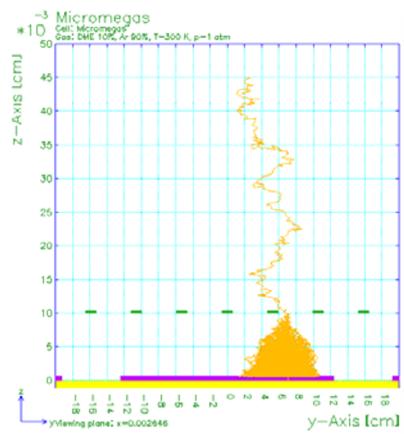

Excellent energy resolution

Electrons drifting from the sensitive volume into the amplication volume with an avalanche in the thin multiplying gap.

MICRO-PATTERN PIXEL DETECTORS

MICRODOT:

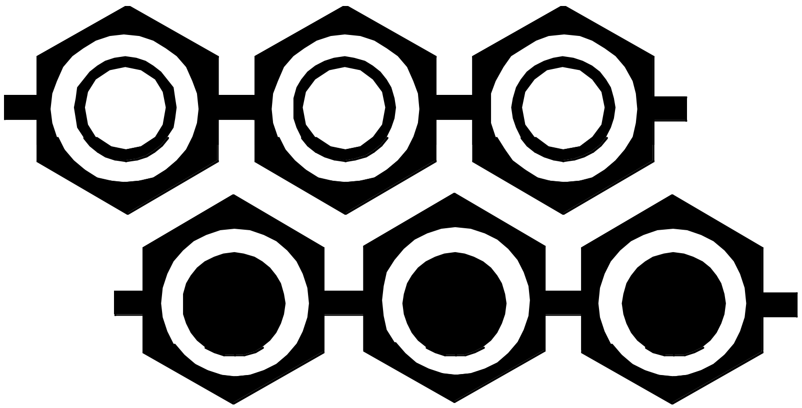

Metal electrodes on silicon

S. Biagi et al
Nucl. Instr. and Meth. A3

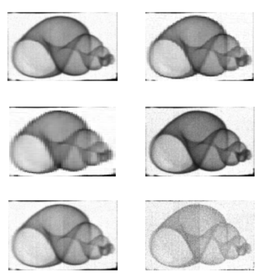

MICRO-PIN ARRAY (MIPA):

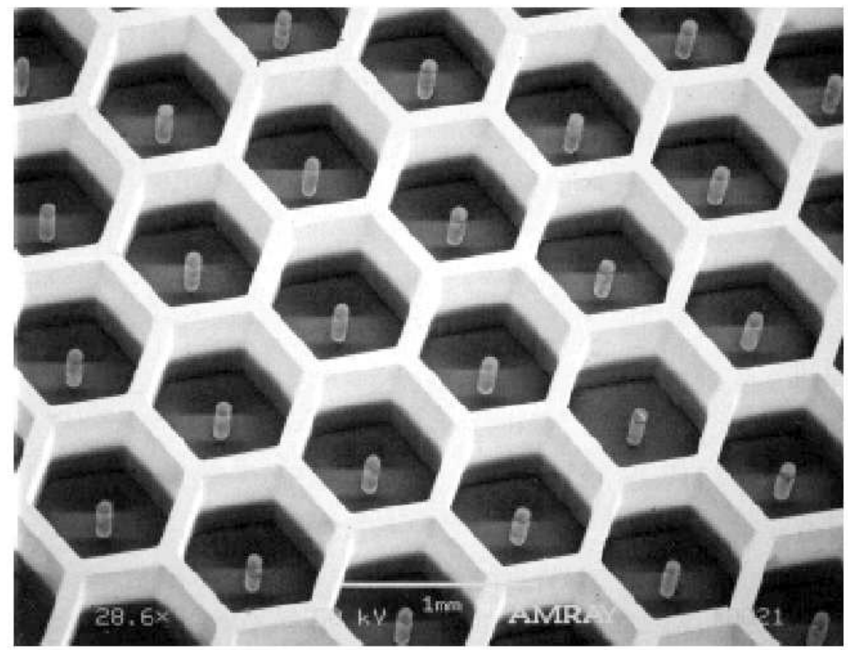

Matrix of individual needle proportional counters
P. Rehak et al, IEEE Trans. Nucl. Sci. NS-47(2000)1426

REVIEW:

Micropattern Gaseous Detectors, Ann. Rev. Nucl. Part. Sci. 49(1999)341

X-ray imaging: Radiology and Diagnostics

13 kV X-ray absorption radiography of a fish bone taken at 2 atm using a GEM + MSGC combination.

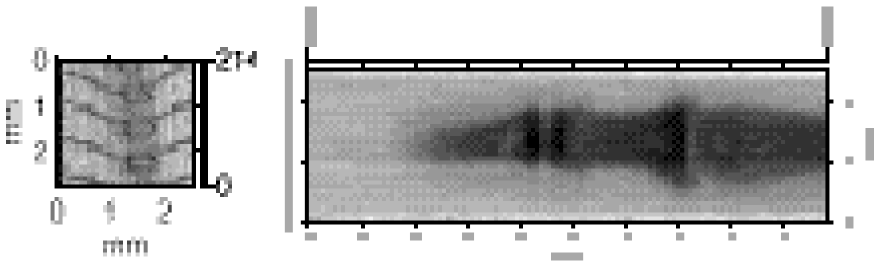

3 mm x 10 mm 50 kV x-ray image of a digit of a mouse.

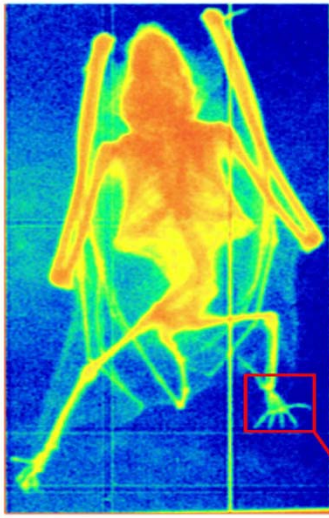

Radiography of a small bat using GEM and 50µm x 50 µm 2d-readout

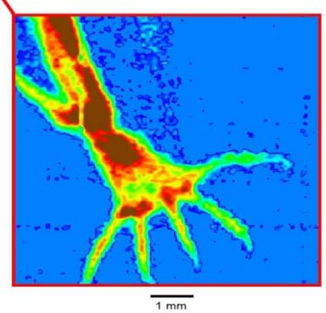

Aging and Long Term Operation

The degradation of operating conditions of wire chambers under sustained irradiation are the main limitation to the use of gas detector in high-energy physics.

'Classical aging effects' are deposits formed on electrode surfaces by chemical reactions in avalanche plasma near the anode.

During gas avalanches many molecules break up and form free radicals (unionized atomic or molecular particles with one or more unsatisfied valence bonds).

Free-radical polymerization is regarded at the dominating mechanism of wire chamber aging

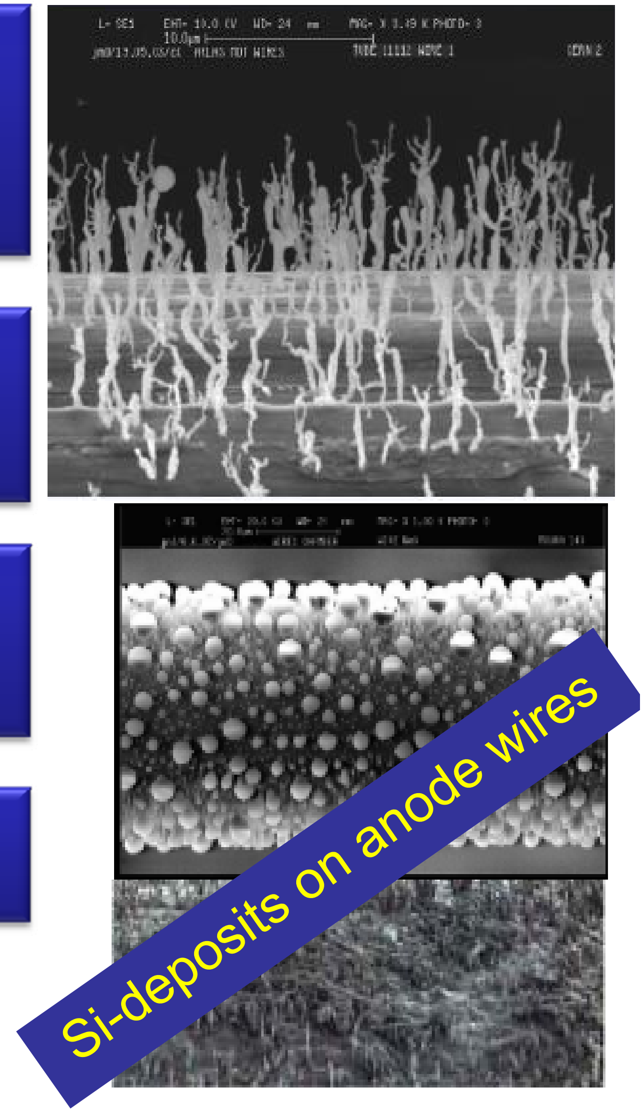

Gas Electron Multiplier (GEM)

Sauli 1996

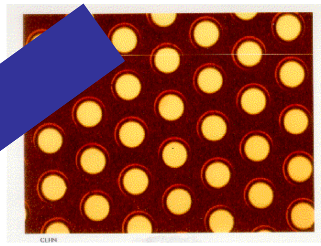

When coupled with a drift electrode above and a readout electrode below, it acts as a micropattern detector.

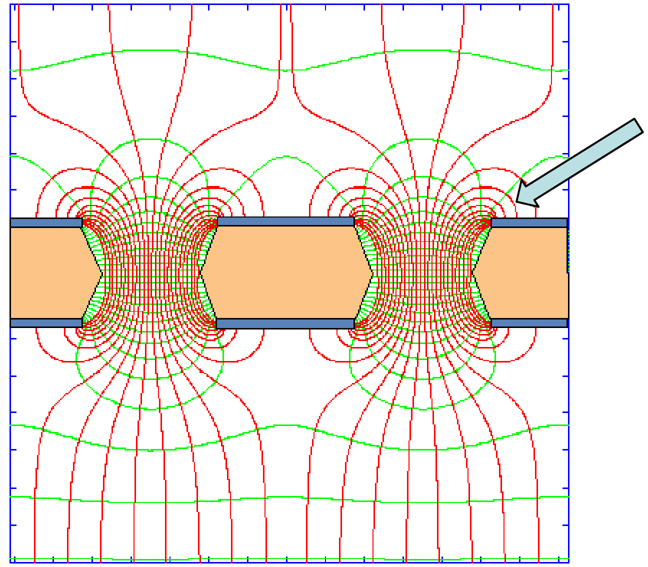

Electric Field

Amplification and detection are decoupled ➔ readout is at zero potential. This permits transfer to a second amplification device and can be coupled to another GEM.

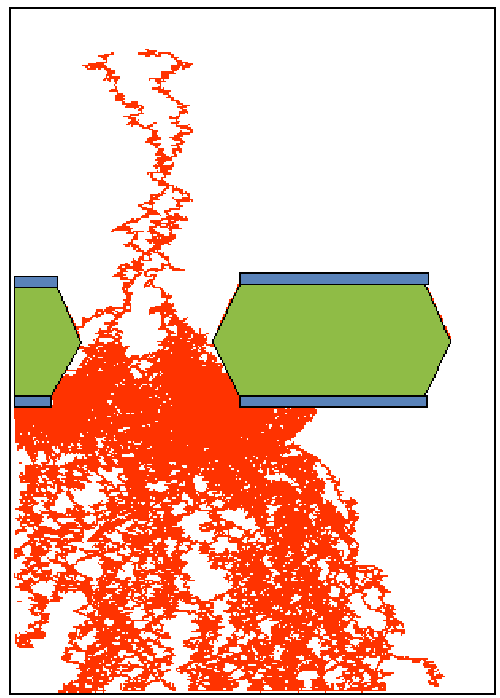

Avalanche across a GEM

Integrated charge per year

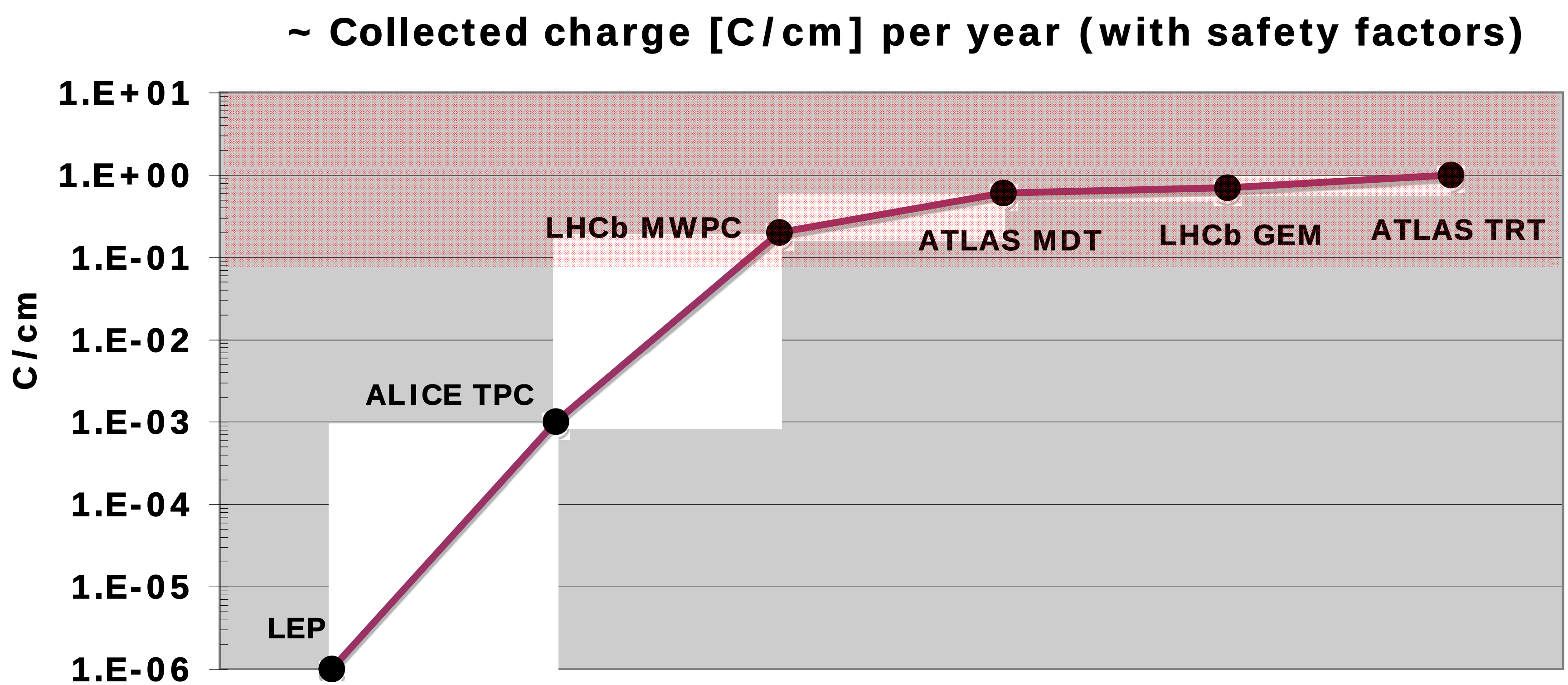

Aging and Long Term Operation - Effects

Leads to the formation of deposits (conducting or insulating) on electrode surfaces.

- Decrease of the gas gain (due to modification of electric field)
- Excessive currents
- Sparking and self-sustained discharges

- Radiation-induced degradation depends on
  - the nature and purity of the gas mixture
  - different additives and trace contaminants
  - materials in contact with the gas
  - materials of the electrodes
  - electric field configuration

The Malter Effect

Microscopic insulating layer deposited on a cathode from quencher dissociation products and/or pollutant molecules.

Strip Damage due to discharges and sparks

Some metal oxide coatings, absorbed layers or even the cathode material itself may not be initially conducting enough →inhibit neutralization of positive ions from the avalanche. These ions generate a strong electric field across the dielectric film and cause electron field-emission at the cathode.

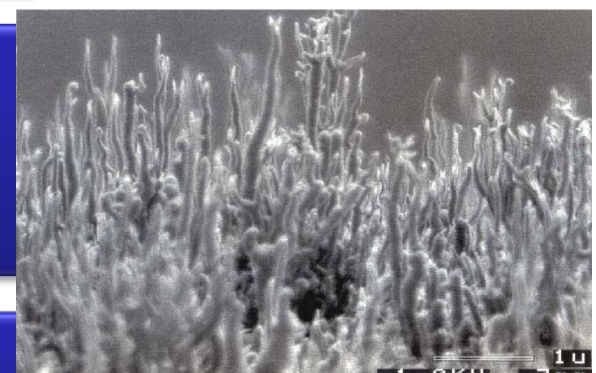

Positive feedback between electron emission at the cathode and anode amplification leads to the appearance of dark current, increased rate of noise pulses and finally exponential current growth (classical Malter breakdown)

Adding water prevents Malter discharges, because water increases the conductivity of partially damaged electrodes

Ionization Density

Detector lifetime depends on ionization density and in turn on the irradiation rate, particle type and energy.

This can be related to the charge density and total energy dissipated in the detector from incoming particles.

Counting rate capabilities are limited by space-charge effects in the avalanches

- gain reduction
- formation of self-quenching streamers

Space-charge effects (at large current densities) reduce the electron energy in the avalanche and thus the ion and radical density in the avalanche plasma.

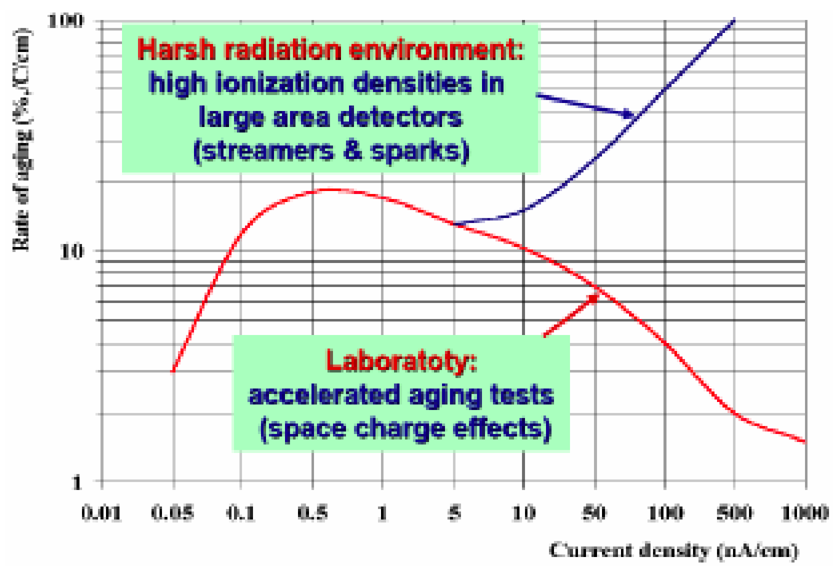

RPC-Aging Imaging of Anodes

Virgin Glass Surface

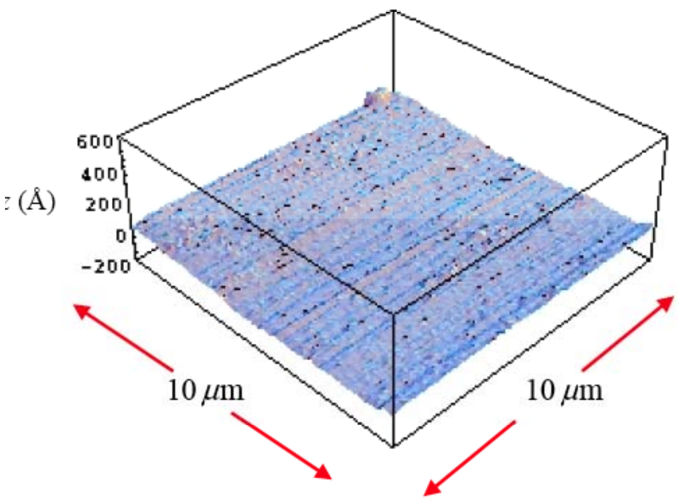

"Good" anode

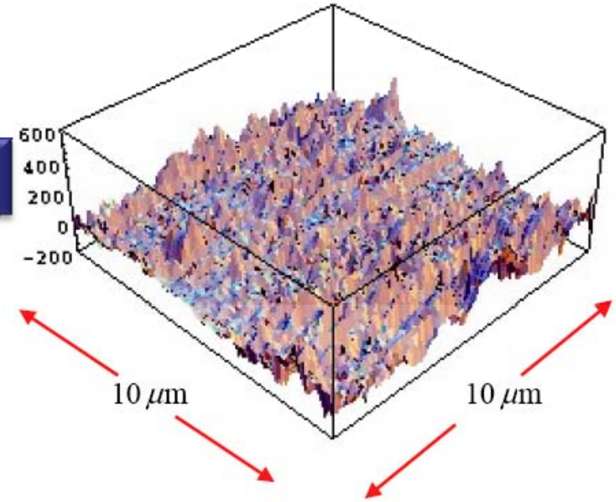

"Bad" anode

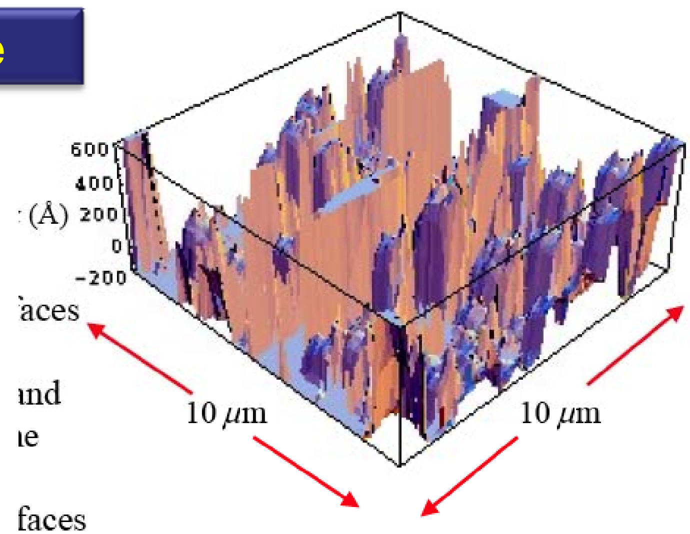

Surfaces etched by HF acid formed from water and Freon in the gas

Aging of BaBar RPCs

The BaBar RPCs were made of Bakelite coated with Linseed oil. A permanent reduction in efficiency was caused by the lack of polymerization in the linseed oil and the formation of oil droplets under the high temperatures and currents.

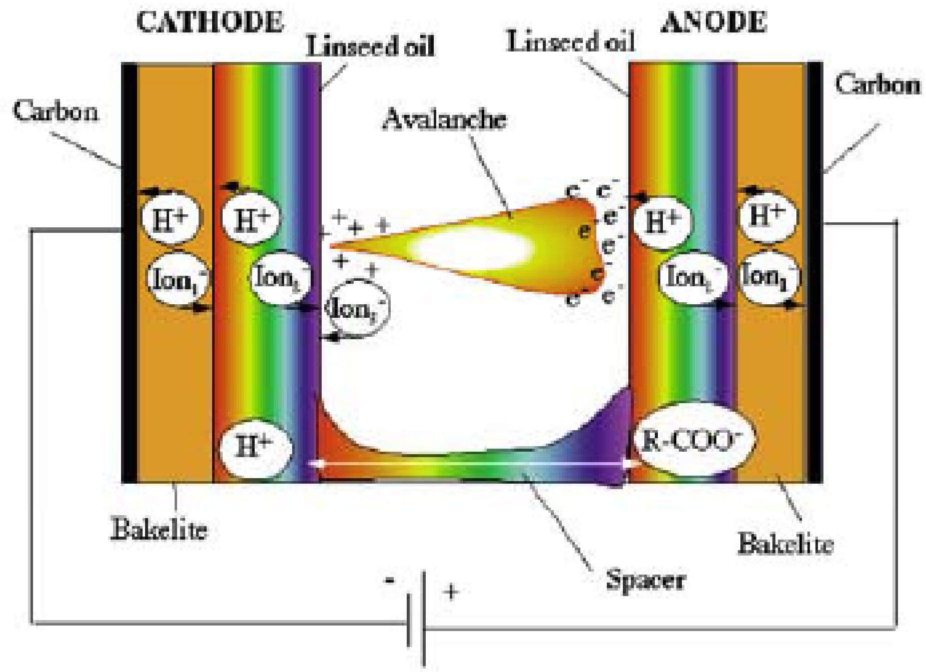

Images of RPC Aging

Damaged Anode

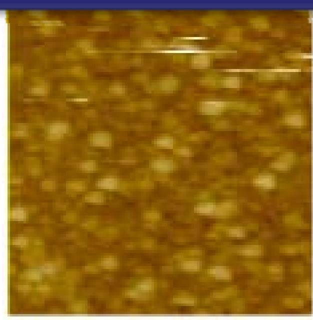

Damaged Cathode

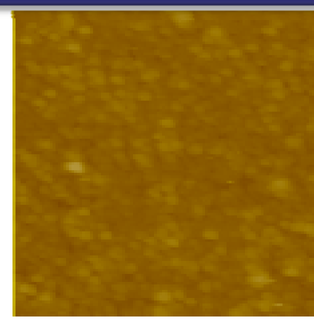

Raw Glass

AFM scans

Damaged Electrode

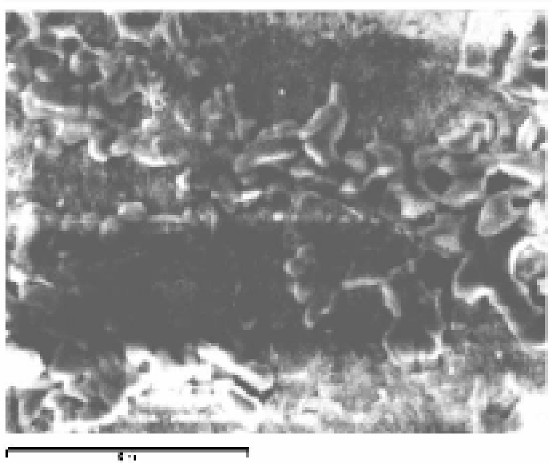

Raw Glass

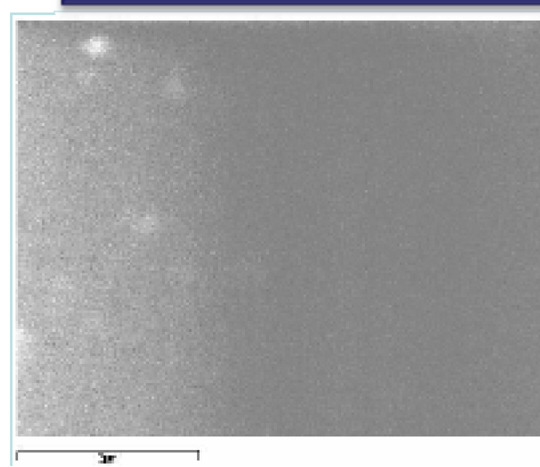

SEM scans

CMS GEM Aging Tests at CERN GIF

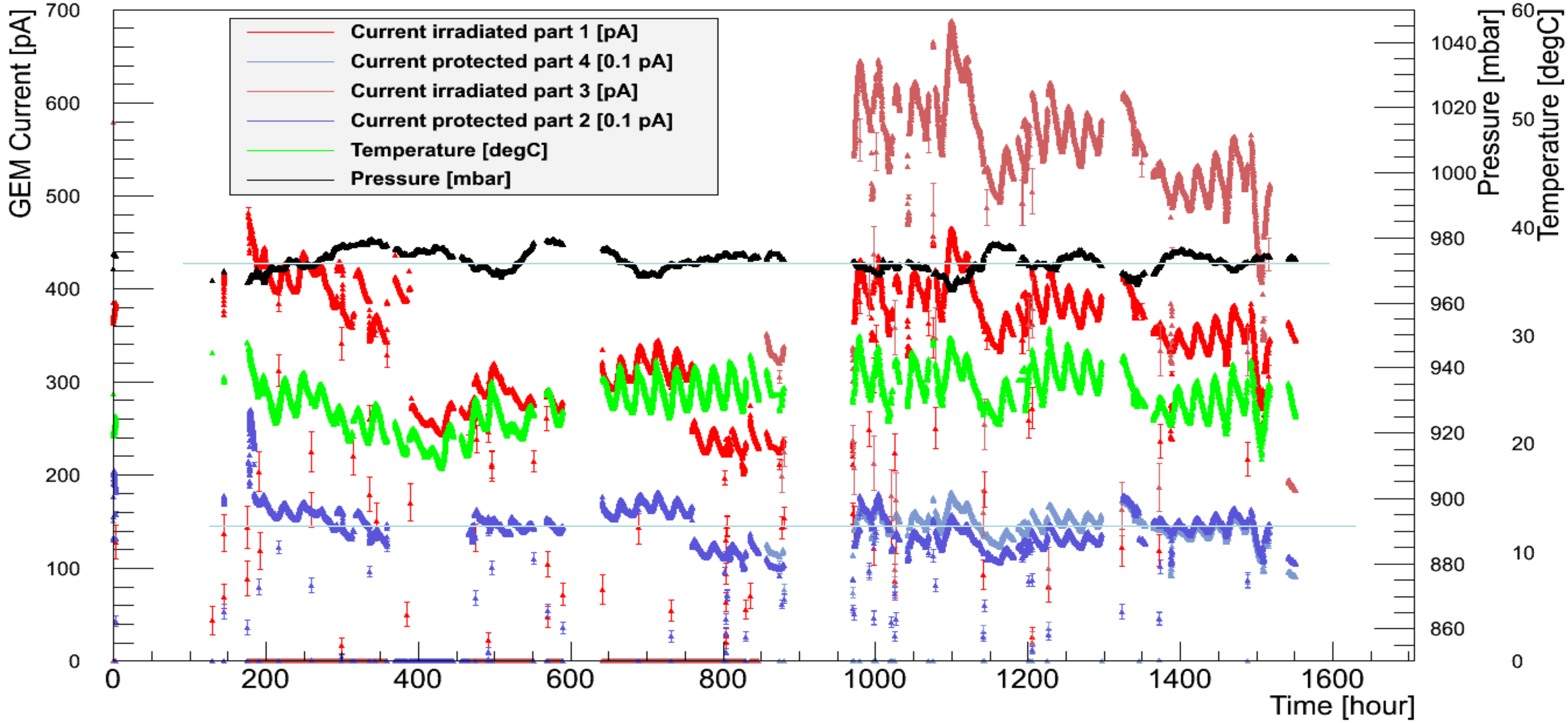

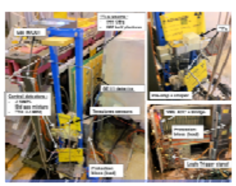

<u>GE1/1 :</u> more that two months of operation -> 9% of the total charge (80mC/cm²).
Two additional pico-ammeters after one month (irradiated+protected sector).
<u>Readout current :</u> protected sector 15x lower than irradiated one (scattering + fluorescence)

J. Merlin

Normalized Corrected Gain for GEM

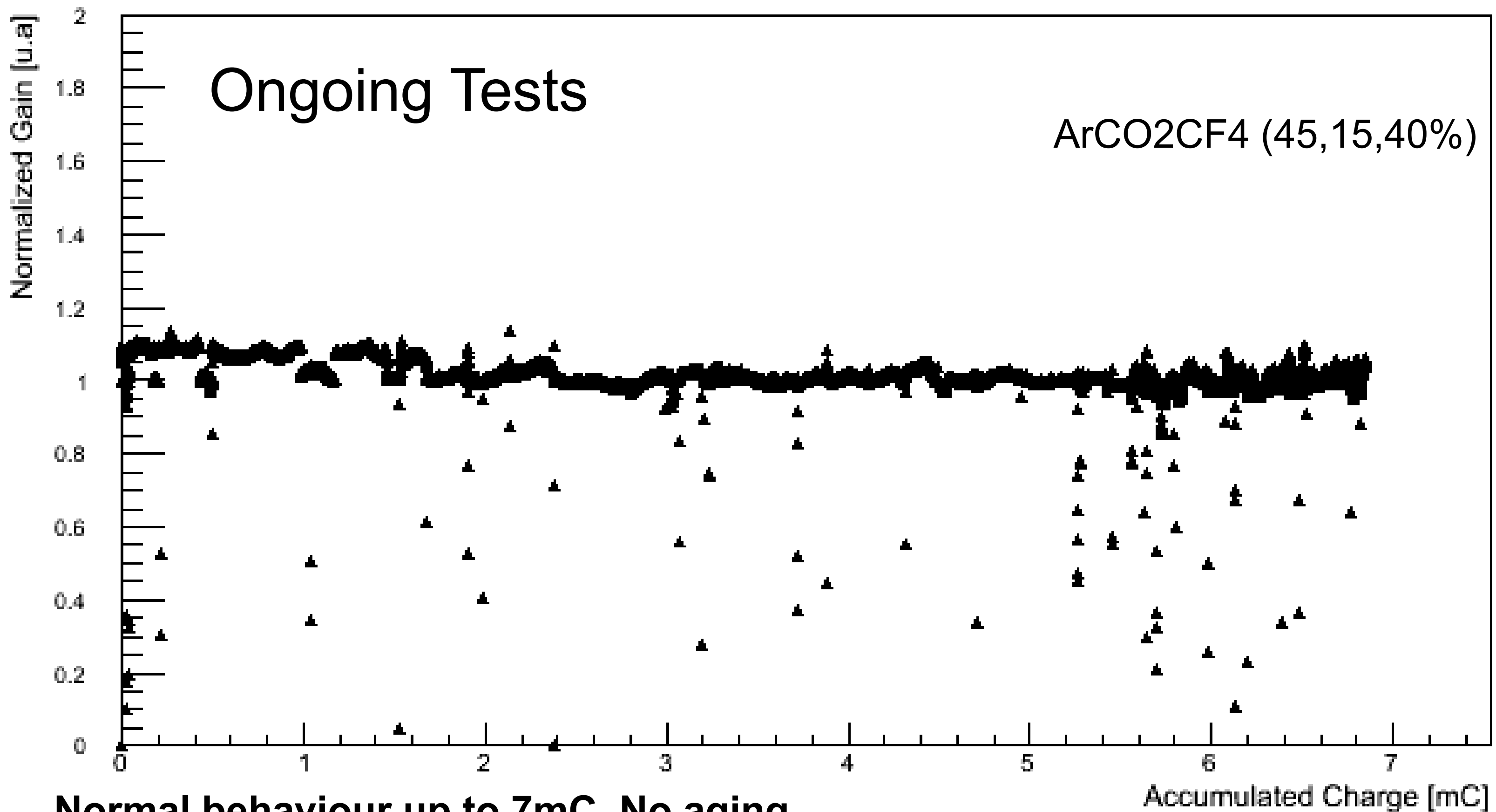

Normal behaviour up to 7mC, No aging

<u>GIF</u> : Good improvement of the efficiency !

-> initially 30-40 %

-> July: 50%

-> August : 90%

J. Merlin

Useful Guidelines for Gaseous Detectors

- Carefully choose construction materials that are radiation hard and have appropriate outgassing properties
- Limited set of aging resistant gases can be used in high intensities experiments: CF_4, $C0_2$,O_2, H_20.
- Validate assembly procedures and ensure maximal cleanliness
- Carefully control any anomalous activity in the detectors: dark currents, changes of anode current and remnant activity in the chamber when the beam goes away
- If aging effects are observed add oxygen-based molecules; operations with CF_4 decreases risk of Si polymerization
- Surface conductivity of electrodes is important because it relates closely to operational capability at high ionization densities

Conclusion and Outlook

- Multiwire chambers have matured since their introduction over the last few decades, with several applications in particle physics and diagnostics of various kinds.
- The last two decades have seen several novel developments in Micropattern Gaseous Detectors.
- Understanding of the discharge mechanisms in these devices has also improved allowing amelioration of their design.
- Progress in manufacture of customized readout boards has evolved revolutionizing the potential applications of these detectors in HEP, radiology, diagnostics, astrophysics and other fields.

Bibliography - 1

[1] Phil. Mag. Xiii(1896)392; Conduction of electricity through gases (Ist ed, 1903); Proc. Of Royal Society, A81(1908)141
[2] G. Charpak et al Nucl. Instr. And Meth. 62(1968)262-268
[3] A. Breskin et al, Nucl. Instr. And Meth 161(1979)19; F. Sauli Physica Scripta 23(1981)526; G. Charpak and F. Sauli Ann. Rev. 34(1984)285, See also C. Grupen, Particle Detectors, Cambridge Press, 1996
[4] E. Babichev et al (1992) Nucl Instrum Methods Phys Res A323: 49, and references therein, S. Baru et al, Novosibirsk Preprint 35(1989) 98-39
[5] G. Kalifa et al, Pediatric. Radiology 28(1998)557
[6] E. Babichev et al in the Proceedings of Frontier Detectors for Frontier Physics Elba, Italy May 2000 & A. Porosev, in Proceeding of Frontier Detector for Frontier Physics, Elba May 2000.
[7] Martinez-Davalos et al, Evaluation of a new low-dose digital x-ray system. Phys Med Biol 38(1993)141
[8] CMS Technical Design Report. CERN/LHCC 98-6
[9] A. Oed, Nucl. Instr. And Meth. A263(1988)35
[10] F. Sauli and A. Sharma, Annual Rev. of Nucl. Sci. 49(1999)41
[11] R. Bouclier et al Nuclear Physics B 61B (1998)315
[12] B. Boimska et al Nuclear Physics B 61B (1998) 498
[13] B. Schmidt , Nucl. Instr. And Meth. A419(1998)230
[14] V. Peskov et al, IEEE Transactions,
Nucl. Sci. NS 45(1998)244
[15] A. Bressan et al Nucl. Instr. And Meth. A 424(1998)321
[16] P. Fonte et al Nucl. Instr. And Meth. A 419(1998) 405
[17] J. Kadyk et al Nuclear Physics B 61B (1998) 258
[18] S.F. Biagi et al, Nucl. Instrum. Methods A371(1995)12
[19] A. Bressan, A. Buzulutskov, L. Ropelewski, F.Sauli and L. Shekhtman, Nucl. Instr. And Meth. A 432(1999)119-124
[20] Y. Giomataris et al Nucl. Instr. And Meth. A 376(1996)29
[21] A. Sharma, ICFA Bulletin Fall 1999 http://www.slac.stanford.edu/pubs/icfa
[22] F. Kuune in Proceeding of Frontier Detector for Frontier Physics, Elba May 2000
[23] F. Bartol et al., J. Phys. III France 6 (1996)337, G. Chaplier et al Nucl. Instr. And Meth A426(1999)
[24] A. Sarvestani et al Nucl. Instr. And Meth. A 419(1998)444
[25] N. Pavel, Siegen, Priv. Com. Oct 2000
[26] F. Sauli Nucl. Instr. And Meth. A 386(1997)531

Bibliography - 2

[27] B. Adeva et al., Nucl. Instr. And Meth A 419(1998)405
[28] P. Rehak et al Proceedings IEEE Nuclear Science Symposium 1999, Seattle USA
[29] W. K. Pitts et al Nucl. Instr. And Meth A438(1999)277
[30] W. K. Pitts See also Proceedings, IEEE Nuclear Science Symposium 1999, Seattle USA
[31] R. Bellazzini et al, Nucl. Instr. And Meth. A 423(1998)125
[32] R. Bellazzini et al, Nucl. Instr. And Meth. A 424(1998)444
[33] C. Richter, PhD. Thesis October 2000 submitted to University of Heidelberg, Germany.
[34] F. Gomez Private Communication and Internal Notes. T. Nunez, and P. Vasquez Theses 1999, Santiago University, Spain.
[35] J. Benlloch et al, IEEE trans NUCl. Sci. NS-45(1998) 234, J. Benlloch et al NIMA 419 (1998) 410
[36] B. Ketzer, Contribution to this Conference
[37] M. Ziegler et al hep-ex/0007007/July 2000, LHC-B Internal Tracking Notes: 99-024, 2000-013, 2000-15, 2000-056, U. Straumann Proceedings, Imaging 2000, Stockholm.
[38] M. Dixit et al, IEEE Trans. 47(1998)809; D. G. Gobbi et al, Phys. Med. Biol. 44(1999)1317
[39] G. Charpak and M. Meynadier Priv. Com. Oct. 2000
[40] M. Dixit in Proceedings of Imaging 2000, Stockholm.
[41] A.Bressan et al Nucl. Instr. And Meth. A 425(1999)254, 262
[42] The future TESLA Linear Collider at DESY Hamburg, DESY 97/048
[43] A. Bressan et al Nucl. Instr. And Meth. A 423(1999)424
[44] A. Sharma, To appear in Nucl. Instr. and Meth. as Proceedings of Symposium on Applications of Particle Detectors in Medicine, Biology and Astrophysics, 5-8 October 1999, Siegen, Germany, also printed as CERN-OPEN-99/373.
[45] S. Ochi et al, SPIE Proceedings 5(1998)324
[46] DIGITAL MAMMOGRAPHY Project MICADO within Weizman, Pisa, Brussels, and Agfa Gaevert.
[47] A. Breskin et al NIM A 442(2000)58
[48] V. Peskov et al NIM A433(1999)492,V. Peskov etal IEEE Trans. Nucl. Science NS-45(1999)244, and contribution to this conference.
[49] A. Sharma CERN Preprint 99/372, Submitted for publication to Nucl. Instr. & Meth. (1999), See also Proceedings of Imaging 2000, Stockholm, June 2000.
[50] C. Richter et al To Appear in the Proceedings of Frontier Detectors for Frontier Physics, Elba 2000.
[51] A.Buzulutskov et al. Nucl. Intr. And Meth A443(2000)164-180, A 433(1999)471, andContribution to Nuclear Science Symposium and Medical Imaging conference, Oct 2000
[52] J. Va'vra Priv. Com. April 2000, and [49]
[53] J.F.C.A. Veloso et al Nucl. Instr. And Meth. A In Press
[54] J.F.C.A.Veloso et al Nuc. Instr. And Meth A In Press
[55] F. Fraga et al, Contribution to Nuclear Science Symposium and Medical Imaging conference, Oct 2000
[56] H. Sakurai et al. "A new type of proportional counter using a capillary plate" NIM A374(1996)341-344,
[57] T.Masuda et al. IEEE Trans NS 47, 2000.
[58] R. Bellazzini et al, Proceedings of Imaging 2000, Stockholm..

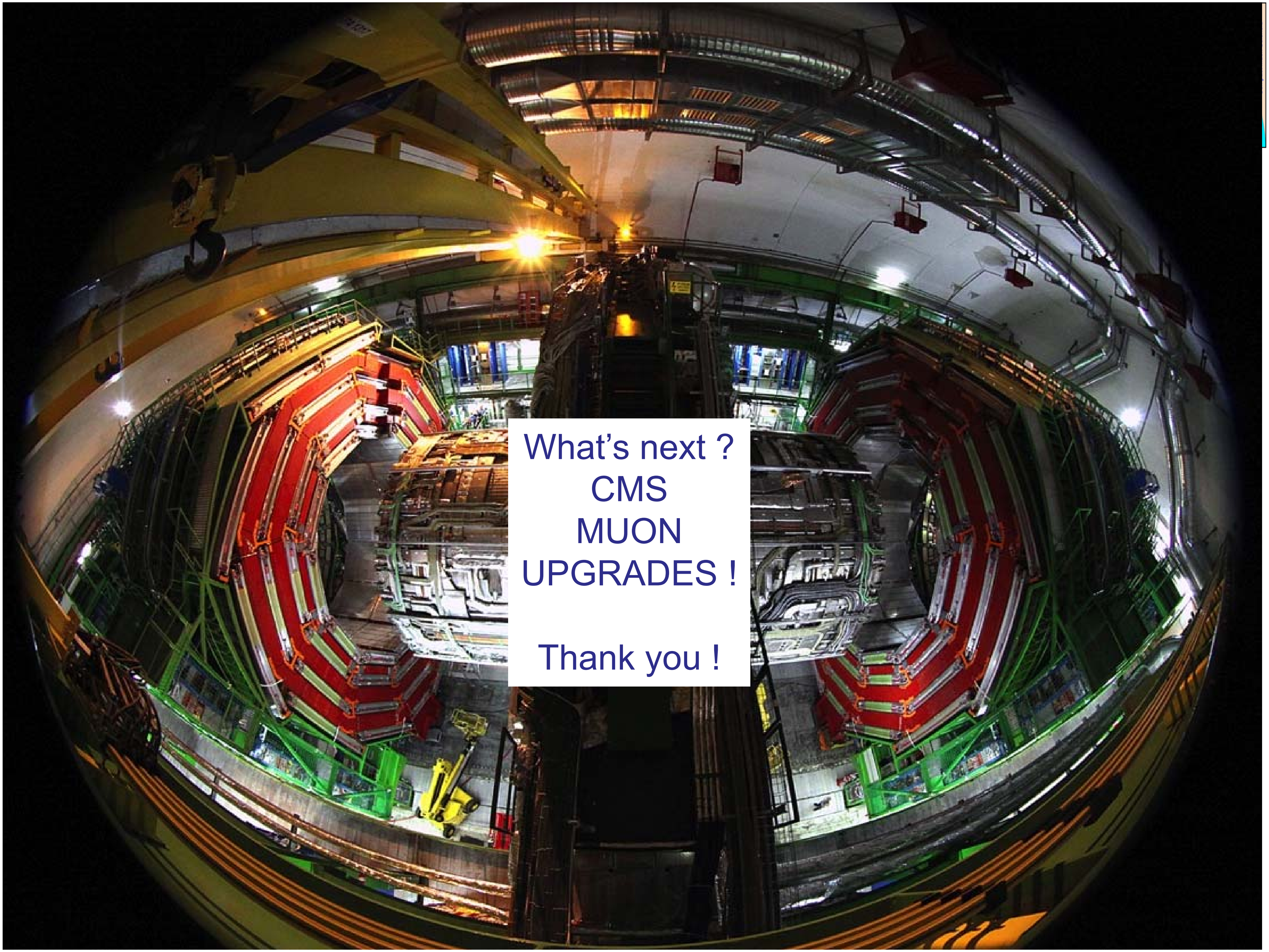
What’s next ?
CMS
MUON
UPGRADES !

Thank you !